JCTC Journal of Chemical Theory and Computation

Article

Cite This: J. Chem. Theory Comput. XXXX, XXX, XXX−XXX

pubs.acs.org/JCTC

Comparison between the Bethe−Salpeter Equation and Configuration Interaction Approaches for Solving a Quantum Chemistry Problem: Calculating the Excitation Energy for Finite 1D Hubbard Chains

Qi Ou[†] and Joseph E. Subotnik*

Department of Chemistry, University of Pennsylvania, Philadelphia, Pennsylvania 19104, United States

ABSTRACT: We calculate the excitation energies of finite 1D Hubbard chains with a variety of different site energies from two perspectives: (i) the physics-based Bethe−Salpeter equation (BSE) method and (ii) the chemistry-based configuration interaction (CI) approach. Results obtained from all methods are compared against the exact values for three classes of systems: metallic, impurity-doped, and molecular (semiconducting/insulating) systems. While in a previous study we showed that the *GW* method holds comparative advantages versus traditional quantum chemistry approaches for calculating the ionization potentials and electron affinities across a large range of Hamiltonians, we show now that the BSE method outperforms CI approaches only for metallic and semiconducting systems. For insulating molecular systems, CI approaches generate better results.

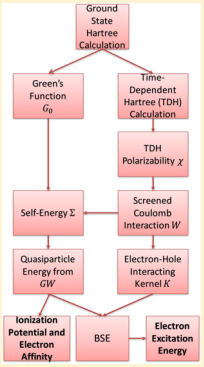

1. INTRODUCTION

In the past few decades, great efforts have been made to explore the excited state properties of various systems via both experimental techniques and computational approaches. Accurate excited state energies are necessary for interpreting electronic spectra, constructing optically active molecules, and designing interfaces between optically active molecules and solid state materials.[1−13]

Obviously, calculating exact excitation energies is impossible for large systems because the Coulomb interaction between electrons makes it exponentially difficult to diagonalize an *N*-body Hamiltonian. As such, we are usually left with approximate schemes. If one is treating isolated molecules, usually the best accuracy is obtained with multireference methods, especially multireference configuration interaction (MRCI).[14−17] That being said, multireference methods are not terribly practical for solid state systems; for solids, single-reference methods are used almost exclusively.

In the literature today, within the context of molecular chemistry, there is a large variety of single-reference methods for excited states. One approach is to use time-dependent density functional theory (TD-DFT) to capture dynamic correlation.[18,19] A second approach is to extend configuration interaction singles (CIS).[20] Even though CIS is unreliable for ordering excited states, CIS is inexpensive and the CIS wave functions are often *qualitatively* correct. To go beyond CIS, several options exist, a few of which we list here:

- Time-dependent Hartree−Fock (TDHF): effectively a full version of CIS that includes electron correlation to the first order.[21]
- CIS(D): a second-order perturbative correction to CIS that is applicable to nondegenerate cases[22,23]
- CC2: the approximate coupled-cluster singles and doubles model that iteratively determines the singles and doubles substitutions as the poles of a true linear response function[24,25]
- ADC(2): algebraic diagrammatic construction through second order[26,27]
- CIS(D_n): a family of quasi-degenerate second-order perturbative corrections to CIS[28]

These single-reference approaches can very often yield qualitatively correct results.

Now, in the context of solid state physics, the methods above have not been considered, either because the starting point for solids is always DFT (and not HF)[13,29−32] or because the methods above were considered too expensive. That being said, in recent years, there has been an explosion of interest in correlated excited state methods based on a Green's function many-body perturbation theory (MBPT).[13,32] The basic idea is to treat correlated electrons (holes) as approximately independent quasiparticles and address all electron−electron correlation effects through the self-energy of the quasiparticle.[33−37] Within MBPT, one can calculate charged excitations with high precision using, for example, Hedin's *GW* approximation[38] and neutral excitations through the Bethe−Salpeter equation (BSE).[39]

In a recent study, for the case of electron attachment and detachment energies, we benchmarked *GW* calculations against configuration interaction (CI) approaches for a set of 1D

Received: March 8, 2017
Published: November 28, 2017

DOI: 10.1021/acs.jctc.7b00246
J. Chem. Theory Comput. XXXX, XXX, XXX−XXX

Hubbard chains.[40] In the present paper, we will now go one step further. For the same model systems, we will benchmark neutral excited state energies as calculated by both the BSE approach (which is popular in the physics community) and a set of CI approaches (which is common in the chemistry community). Exact excitation energies are obtained using direct diagonalization of the full Hamiltonian so that the approximate results can be evaluated for accuracy.

An outline of this paper is as follows. In section 2, we review BSE theory by deriving the relevant equations using standard quantum chemistry notation (section 2.A). Then we review the relevant CI theory (section 2.B) and our choice of model system (section 2.C). In section 3, we present the excitation energies predicted by these different methods. In section 4, we discuss various factors that influence the performance of the BSE methods. In section 5, we conclude.

Unless otherwise specified, we use lowercase latin letters to denote spin molecular orbitals (MOs) (a, b, c, d for virtual orbitals, i, j, k, l, m for occupied orbitals, p, q, r, s, w for arbitrary orbitals) and Greek letters (α, β, γ, δ, λ, σ, μ, ν) to denote atomic orbitals (AOs). Position is denoted by $\mathbf{r}$, and position/spin together are denoted by $\mathbf{x} \equiv (\mathbf{r},\sigma)$. Thus, the notation $\phi_a(\mathbf{x})$ signifies an one-electron spin wave function indexed by "a", where the spin of ϕ_a equals the spin of $\mathbf{x}$. The electronic excited states obtained within the random-phase approximation (RPA) are denoted by Ψ_I or Ψ_J (with uppercase latin indices I, J).

2. THEORY

We will now review both BSE theory and the relevant CI theory. Because BSE is less common in chemistry than is CI, we will focus especially on deriving the relevant equations for BSE (which takes some time) using the standard quantum chemistry notation. We will assume only basic familiarity with Green's function formalisms, though we will assume some of the basic results of ref 40 (which summarizes the GW approach in the language of quantum chemistry). For BSE, we will follow Strinati's paper (ref 41) in detail and make a flowchart to make the process easily repeatable. Note that Strinati's paper derives the BSE working equations only in the Tamm−Dancoff approximation, and thus, we will modify the derivation slightly. Below, we will also highlight the three key assumptions of BSE theory.

2.A. Bethe−Salpeter Equation. *2.A.1. Two-Particle Correlation Function and Its BSE.* BSE is derived using standard MBPT and the language of Green's functions. We suppose that $|N\rangle$ is the exact fully interacting ground state of the N-body electronic system. Our final result agrees with Louie's result in ref 35. We define the one- and two-particle Green's function as

$$G_1(1, 1') \equiv -\mathrm{i}/\hbar\langle N|T[\hat{\Psi}(1)\hat{\Psi}^\dagger(1')]|N\rangle \tag{1}$$

$$G_2(12; 1'2') \equiv (-\mathrm{i}/\hbar)^2\langle N|T[\hat{\Psi}(1)\hat{\Psi}(2)\hat{\Psi}^\dagger(2')\hat{\Psi}^\dagger(1')]|N\rangle \tag{2}$$

Here we use the simplified notation for the indices $(\mathbf{x}_1, t_1) = (\mathbf{r}_1, \sigma_1, t_1) \rightarrow (1)$, $(\mathbf{x}_2, t_2) = (\mathbf{r}_2, \sigma_2, t_2) \rightarrow (2)$, i.e., (1) and (2) denote both space and time. We use the standard notation $\int \mathrm{d}\mathbf{x}_1 = \sum_{\sigma_1}\int \mathrm{d}\mathbf{r}_1$. T denotes time-ordering. The two-particle correlation function is defined as[41]

$$L(12; 1'2') \equiv G_1(1, 1')G_1(2, 2') - G_2(1, 2; 1', 2') \tag{3}$$

Now, invoking a well-known trick in Green's function theory, we imagine applying a one-particle potential $\tilde{u}(\mathbf{x}, \mathbf{x}'; t)$ to the electronic system. According to well-known functional derivative identities,[41] one can show that (for $t'_2 = t_2 + \delta$)

$$L(12; 1'2') = \frac{\delta G(1, 1')}{\delta\tilde{u}(\mathbf{x}_2, \mathbf{x}'_2; t_2)} \tag{4a}$$

See Appendix A for a proof of this identity. Furthermore, if we define the quantity $u(\mathbf{x}_1, t_1; \mathbf{x}_2, t_2) = \tilde{u}(\mathbf{x}_1, \mathbf{x}_2; t_2)\delta(t_1 - t_2)$, we can also take a formal derivative of G with respect to u, and we find

$$L(12; 1'2') = \frac{\delta G_1(1, 1')}{\delta u(2, 2')} \tag{4b}$$

See again Appendix A.

Although eq 4b is applicable only when $t_2 = t'_2$, a diagrammatic analysis shows that the BSE (as presented in eq 12) is in fact applicable for $t_2 \neq t'_2$.[41] That being said, for the present paper, we note that we will eventually set $t'_2 = t_2 + \delta$ (after eq 26); we will use eq 4b only as a formal tool to manipulate L and derive the BSE more quickly. Thus, applying the matrix identity $\frac{\delta A^{-1}}{\delta x} = -A^{-1}\frac{\delta A}{\delta x}A^{-1}$, we can rewrite $L(12; 1'2')$ as

$$L(12; 1'2') = -\iint \mathrm{d}3\ \mathrm{d}3'\ G_1(1, 3)\frac{\delta G_1^{-1}(3, 3')}{\delta u(2', 2)}G_1(3', 1') \tag{5}$$

We must now evaluate eq 5. When using Green's functions, one always distinguishes between the Green's function for the interacting Hamiltonian and the Green's function for the noninteracting Hamiltonian (which can be easily distinguished). The relationship between the noninteracting Green's function $G_1^{(0)}$ and the exact Green's function G_1 is

$$G_1^{-1}(1, 2) = G_1^{(0)-1}(1, 2) - u(1, 2) - \Sigma(1, 2) \tag{6}$$

where $\Sigma(1, 2)$ denotes the self-energy (which is defined by eq 6). For BSE, the first approximation (*Approximation #1*) is to invoke GW theory for single particles, so that the self-energy in eq 6 contains the contribution from two parts

$$\Sigma(1, 2) \equiv \Sigma^{\mathrm{H}}(1, 2) + \Sigma^{\mathrm{GW}}(1, 2) \tag{7}$$

Here

$$\Sigma^{\mathrm{H}}(1, 2) = \delta(1, 2)\left[-\mathrm{i}\hbar\int \mathrm{d}3\ v(1, 3)G_1(3, 3^+)\right] \tag{8}$$

denotes the Hartree contribution (i.e., the mean-field Coulombic effect of all electrons together), and

$$\Sigma^{\mathrm{GW}}(1, 2) = \mathrm{i}\hbar G_1(1, 2)W(1^+, 2) \tag{9}$$

captures the correlated motion of an individual electron in a sea of other electrons that results in the electronic screening of the mean-field potential; the screening potential W is computed approximately via a GW calculation. The notation $A(1^+, 2)$ signifies that time t_1 should be replaced by $t_1 + \delta$. In eqs 6−9, we note that for nonzero matrix elements, we require that (1) and (2) should have the same spin.

At this point, we plug eq 6 into eq 5, and we find

DOI: 10.1021/acs.jctc.7b00246
J. Chem. Theory Comput. XXXX, XXX, XXX−XXX

$$L(12;\,1'2') = \iiint \mathrm{d3}\;\mathrm{d3'}\; G_1(1,\,3)\left[\delta(2',\,3)\delta(2,\,3') + \frac{\delta\Sigma(3,\,3')}{\delta u(2',\,2)}\right]G_1(3',\,1') \tag{10}$$

$$= G_1(1,\,2')G_1(2,\,1') + \iiiint \mathrm{d3}\;\mathrm{d3'}\;\mathrm{d4}\;\mathrm{d4'}\; G_1(1,\,3)G_1(3',\,1')\frac{\delta\Sigma(3,\,3')}{\delta G_1(4,\,4')}\frac{\delta G_1(4,\,4')}{\delta u(2',\,2)} \tag{11}$$

$$= G_1(1,\,2')G_1(2,\,1') + \iiiint \mathrm{d3}\;\mathrm{d3'}\;\mathrm{d4}\;\mathrm{d4'}\; G_1(1,\,3)G_1(3',\,1')\frac{\delta\Sigma(3,\,3')}{\delta G_1(4,\,4')}L(42;\,4'2') \tag{12}$$

Equation 12 is the BSE for L. If we define the electron−hole interaction kernel K as[41]

$$K(34';\,3'4) \equiv \frac{\delta\Sigma(3,\,3')}{\delta G_1(4,\,4')} \tag{13}$$

the BSE for L can then be written as

$$L(12;\,1'2') = G_1(1,\,2')G_1(2,\,1') + \iiiint \mathrm{d3}\;\mathrm{d3'}\;\mathrm{d4}\;\mathrm{d4'}\; G_1(1,\,3)G_1(3',\,1')K(34';\,3'4)L(42;\,4'2') \tag{14}$$

If one plugs eq 7 into eq 13 (with the help of eqs 8 and 9) and neglects the derivative of the screened interaction W with respect to G (which constitutes Approximation #2 for BSE), K can be rewritten approximately as

$$K(34';\,3'4) = -\mathrm{i}\hbar\delta(3,\,3')\delta(4^+,\,4')v(3,\,4) + \mathrm{i}\hbar\delta(3,\,4)\delta(3',\,4')W(3^+,\,3') \tag{15}$$

$$\equiv K^x(34';\,3'4) + K^d(34';\,3'4) \tag{16}$$

In a confusing twist of notation, the first term K^x, which results from the Coulomb potential in eq 13, is usually called the exchange term, while the second term K^d, which results from the screened-exchange self-energy in eq 13, is usually called the direct interaction term.

2.A.2. Eigenvalue Problem for BSE. The derivation of the effective eigenvalue problem for BSE starts from the analysis of the four time variables in the two-body Green's function $G(12;\,1'2')$ (i.e. the second term in $L(12;\,1'2')$ in eq 3). To begin this analysis, one considers a change of variables to

$$\tau_1 \equiv t_1 - t_{1'} \qquad \tau_2 \equiv t_2 - t_{2'} \qquad \tau \equiv \tilde{t}_1 - \tilde{t}_2 \tag{17}$$

where $\tilde{t}_1 = \frac{1}{2}(t_1 + t_{1'})$ and $\tilde{t}_2 = \frac{1}{2}(t_2 + t_{2'})$. The particle−hole Green's function contains six classes as follows (with the order of the time variables for each class of the Green's function shown in Figure 1)

$$G_2^{\mathrm{I}}(12;\,1'2') = (-\mathrm{i}/\hbar)^2\langle N|T[\hat{\Psi}(1)\hat{\Psi}^\dagger(1')]T[\hat{\Psi}(2)\hat{\Psi}^\dagger(2')]|N\rangle\cdot \theta\left(\tau - \frac{1}{2}|\tau_1| - \frac{1}{2}|\tau_2|\right) \tag{18}$$

$$G_2^{\mathrm{II}}(12;\,1'2') = (-\mathrm{i}/\hbar)^2\langle N|T[\hat{\Psi}(2)\hat{\Psi}^\dagger(2')]T[\hat{\Psi}(1)\hat{\Psi}^\dagger(1')]|N\rangle\cdot \theta\left(-\tau - \frac{1}{2}|\tau_1| - \frac{1}{2}|\tau_2|\right) \tag{19}$$

$$G_2^{\mathrm{III}}(12;\,1'2') = -(-\mathrm{i}/\hbar)^2\langle N|T[\hat{\Psi}(2)\hat{\Psi}^\dagger(1')]T[\hat{\Psi}(1)\hat{\Psi}^\dagger(2')]|N\rangle\cdot \theta\left(\frac{\tau_2}{2} - \frac{\tau_1}{2} - \frac{1}{2}\left|-\tau + \frac{\tau_1}{2} + \frac{\tau_2}{2}\right| - \frac{1}{2}\left|\tau + \frac{\tau_1}{2} + \frac{\tau_2}{2}\right|\right) \tag{20}$$

$$G_2^{\mathrm{IV}}(12;\,1'2') = -(-\mathrm{i}/\hbar)^2\langle N|T[\hat{\Psi}(1)\hat{\Psi}^\dagger(2')]T[\hat{\Psi}(2)\hat{\Psi}^\dagger(1')]|N\rangle\cdot \theta\left(\frac{\tau_1}{2} - \frac{\tau_2}{2} - \frac{1}{2}\left|-\tau + \frac{\tau_2}{2} + \frac{\tau_1}{2}\right| - \frac{1}{2}\left|\tau + \frac{\tau_2}{2} + \frac{\tau_1}{2}\right|\right) \tag{21}$$

$$G_2^{\mathrm{V}}(12;\,1'2') = (-\mathrm{i}/\hbar)^2\langle N|T[\hat{\Psi}(1)\hat{\Psi}(2)]T[\hat{\Psi}^\dagger(2')\hat{\Psi}^\dagger(1')]|N\rangle\cdot \theta\left(\frac{\tau_1}{2} + \frac{\tau_2}{2} - \frac{1}{2}\left|\tau + \frac{\tau_2}{2} - \frac{\tau_1}{2}\right| - \frac{1}{2}\left|\tau + \frac{\tau_2}{2} - \frac{\tau_1}{2}\right|\right) \tag{22}$$

$$G_2^{\mathrm{VI}}(12;\,1'2') = (-\mathrm{i}/\hbar)^2\langle N|T[\hat{\Psi}^\dagger(2')\hat{\Psi}^\dagger(1')]T[\hat{\Psi}(1)\hat{\Psi}(2)]|N\rangle\cdot \theta\left(-\frac{\tau_1}{2} - \frac{\tau_2}{2} - \frac{1}{2}\left|\tau + \frac{\tau_2}{2} - \frac{\tau_1}{2}\right| - \frac{1}{2}\left|\tau + \frac{\tau_2}{2} - \frac{\tau_1}{2}\right|\right) \tag{23}$$

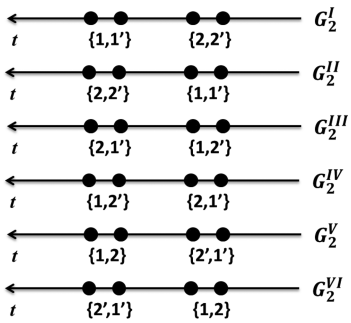

Figure 1. Schematic graph of the time ordering for the two-body Green's function. Note that the time order for the electrons and/or holes within the same curly brace is random. Each class of the Green's function therefore has four different time combinations, making a total of 24 terms in the two-body Green's function. The time increases from right to left.

It is clear that from the combination of the creation and annihilation operators that $G_2^{\mathrm{I-IV}}$ correspond to the electron−hole portion of the two-body Green's function (i.e., one electron and one hole are being propagated in the N-body system). G_2^{V} and G_2^{VI} correspond to the electron−electron and hole−hole portion of the two-body Green's function, respectively, which do not involve the excitation energies of the N-body system (but rather the $(N \pm 2)$-body system). Thus, to locate the excited states of the N-body system, one needs to consider only $G_2^{\mathrm{I-IV}}$.

To construct the eigenvalue equation for BSE, one performs a Fourier transform on both sides of eq 14. Here we take $G_2^{\mathrm{I}}(12;\,1'2')$ as an example to compute the Fourier transform results. First we define the right- and left-hand electron−hole amplitudes as

DOI: 10.1021/acs.jctc.7b00246
J. Chem. Theory Comput. XXXX, XXX, XXX−XXX

$$\chi_S^{eh}(\mathbf{x}_1, \mathbf{x}_2; t_1 - t_2) \equiv \langle N|T[\hat{\Psi}(1)\hat{\Psi}^{\dagger}(2)]N_S\rangle \exp[i(E_S - E_0)(t_1 + t_2)/2\hbar] \quad (24)$$

$$\tilde{\chi}_S^{eh}(\mathbf{x}_1, \mathbf{x}_2; t_1 - t_2) \equiv \langle N_S|T[\hat{\Psi}(1)\hat{\Psi}^{\dagger}(2)]N\rangle \exp[-i(E_S - E_0)(t_1 + t_2)/2\hbar] \quad (25)$$

where $|N_S\rangle$ denotes the Sth excited state of the N-body system.[42] Then $G_2^{I}(12; 1'2')$ can be rewritten as

$$G_2^{I}(12; 1'2') = (-i/\hbar)^2 \sum_S \exp[i(E_0 - E_S)\tau/\hbar]\chi_S^{eh}(\mathbf{x}_1, \mathbf{x}_{1'}; \tau_1) \times \tilde{\chi}_S^{eh}(\mathbf{x}_2, \mathbf{x}_{2'}; \tau_2)\cdot\theta\left(\tau - \frac{1}{2}|\tau_1| - \frac{1}{2}|\tau_2|\right) \quad (26)$$

Second, upon setting $t_{2'} = t_2 + \delta(\delta \to 0^+)$ (which gives $\tau_2 = -\delta$ and $\tau = \tilde{t}_1 - t_2$) and Fourier transforming the variable t_2, the result given by $G_2^{I}(12; 1'2')$ can be evaluated as

$$\int_{-\infty}^{+\infty} dt_2\, e^{-i\omega t_2} G_2^{I}(12; 1'2') = \int_{-\infty}^{+\infty} dt_2\, e^{-i\omega t_2}(-i/\hbar)^2\theta\left(\tilde{t}_1 - t_2 - \frac{1}{2}|\tau_1|\right) \times \sum_S e^{i(E_0 - E_S)(\tilde{t}_1 - t_2)/\hbar}\chi_S^{eh}(\mathbf{x}_1, \mathbf{x}_{1'}; \tau_1)\tilde{\chi}_S^{eh}(\mathbf{x}_2, \mathbf{x}_{2'}; -\delta) \quad (27)$$

$$= \left(\frac{-i}{\hbar}\right)^2 \int_{-\infty}^{\tilde{t}_1 - (1/2)|\tau_1|} dt_2\, e^{-i\omega t_2} \times \sum_S e^{i(E_0 - E_S)(\tilde{t}_1 - t_2)/\hbar}\chi_S^{eh}(\mathbf{x}_1, \mathbf{x}_{1'}; \tau_1)\tilde{\chi}_S^{eh}(\mathbf{x}_2, \mathbf{x}_{2'}; -\delta) \quad (28)$$

$$= -\frac{i}{\hbar} e^{-i[\omega\tilde{t}_1 - (\hbar\omega - E_S + E_0)(|\tau_1|/2\hbar)]} \cdot \sum_S \frac{\chi_S^{eh}(\mathbf{x}_1, \mathbf{x}_{1'}; \tau_1)\tilde{\chi}_S^{eh}(\mathbf{x}_2, \mathbf{x}_{2'}; -\delta)}{\hbar\omega - (E_S - E_0) + i\eta} \quad (29)$$

An imaginary infinitesimal has been included in the denominator of eq 29 to ensure the convergence of the integral. Performing the same transformation for G_2^{I-IV}, one finds that the electron−hole correlation function (eq 3) in the frequency domain $L^{eh}(\mathbf{x}_1, \mathbf{x}_2; \mathbf{x}_{1'}, \mathbf{x}_{2'}|t_1, t_{1'}; \omega)$ contains only the contributions from $G_2^{I}(12; 1'2')$ and $G_2^{II}(12; 1'2')$.[43] Thus

$$L^{eh}(\mathbf{x}_1, \mathbf{x}_2; \mathbf{x}_{1'}, \mathbf{x}_{2'}|t_1, t_{1'}; \omega) = -\int_{-\infty}^{+\infty} dt_2\cdot e^{-i\omega t_2}[G_2^{I}(12; 1'2') + G_2^{II}(12; 1'2')] \quad (30)$$

$$= \frac{i}{\hbar} e^{-i(E_S - E_0)|\tau_1|/2\hbar}\left[e^{-i\omega(\tilde{t}_1 - (|\tau_1|/2))} \cdot \sum_S \frac{\chi_S^{eh}(\mathbf{x}_1, \mathbf{x}_{1'}; \tau_1)\tilde{\chi}_S^{eh}(\mathbf{x}_2, \mathbf{x}_{2'}; -\delta)}{\hbar\omega - (E_S - E_0) + i\eta} - e^{-i\omega(\tilde{t}_1 + (|\tau_1|/2))} \cdot \sum_S \frac{\chi_S^{eh}(\mathbf{x}_2, \mathbf{x}_{2'}; \delta)\tilde{\chi}_S^{eh}(\mathbf{x}_1, \mathbf{x}_{1'}; -\tau_1)}{\hbar\omega + (E_S - E_0) - i\eta}\right] \quad (31)$$

Note that the first term in eq 3, the product of one-body Green's functions, does not contribute because its transform vanishes when ω is nonzero. Thus, eq 31 gives the Fourier transform for the left-hand side of eq 14. Performing the same Fourier transform on the right-hand side of eq 14 gives[56] (with $\tilde{t}_4 = \frac{t_4 + t_4'}{2}$ and $\tau_4 = t_4 - t_4'$)

$$\frac{i}{\hbar}\iiint d3\, d3'\, d4\, d4'\, G_1(1, 3)G_1(3', 1')K(34'; 3'4)e^{-i(E_S - E_0)|\tau_4|/2\hbar}\left[e^{-i\omega(\tilde{t}_4 - (|\tau_4|/2))} \cdot \sum_S \frac{\chi_S^{eh}(\mathbf{x}_4, \mathbf{x}_{4'}; \tau_4)\tilde{\chi}_S^{eh}(\mathbf{x}_2, \mathbf{x}_{2'}; -\delta)}{\hbar\omega - (E_S - E_0) + i\eta} - e^{-i\omega(\tilde{t}_4 + (|\tau_4|/2))} \cdot \sum_S \frac{\chi_S^{eh}(\mathbf{x}_2, \mathbf{x}_{2'}; \delta)\tilde{\chi}_S^{eh}(\mathbf{x}_4, \mathbf{x}_{4'}; -\tau_4)}{\hbar\omega + (E_S - E_0) - i\eta}\right] \quad (32)$$

Evaluating the residue of eqs 31 and 32 at a particular pole $\hbar\omega = (E_S - E_0) \equiv \Omega_S$, one has

$$\chi_S^{eh}(\mathbf{x}_1, \mathbf{x}_{1'}; \tau_1)e^{-i\Omega_S\tilde{t}_1/\hbar} = \iiint d3\, d3'\, d4\, d4'\, G_1(1, 3)G_1(3', 1') \times K(34'; 3'4)\chi_S^{eh}(\mathbf{x}_4, \mathbf{x}_{4'}; \tau_4)e^{-i\Omega_S\tilde{t}_4/\hbar} \quad (33)$$

We now perform a series of transformations upon eq 33 in order to get the final working equations:

1. Plug the expression of K (eq 15) into eq 33, which gives

$$\chi_S^{eh}(\mathbf{x}_1, \mathbf{x}_{1'}; \tau_1)e^{-i\Omega_S\tilde{t}_1/\hbar} = i\hbar\iiint d3\, d3'\, d4\, d4'\, G_1(1, 3)G_1(3', 1')[-\delta(3, 3')\delta(4^+, 4')v(3, 4) + \delta(3, 4)\delta(3', 4')W(3^+, 3')]\chi_S^{eh}(\mathbf{x}_4, \mathbf{x}_{4'}; \tau_4)e^{-i\Omega_S\tilde{t}_4/\hbar} \quad (34)$$

$$= -i\hbar\iint d3\, d3'\, G_1(1, 3)G_1(3,1')v(3, 3')\chi_S^{eh}(\mathbf{x}_{3'}, \mathbf{x}_{3'}; -\delta)e^{-i\Omega_S\tilde{t}_3/\hbar} + i\hbar\iint d3\, d3'\, G_1(1, 3)G_1(3', 1')W(3^+, 3')\chi_S^{eh}(\mathbf{x}_3, \mathbf{x}_{3'}; \tau_3)e^{-i\Omega_S\tilde{t}_3/\hbar} \quad (35)$$

DOI: 10.1021/acs.jctc.7b00246
J. Chem. Theory Comput. XXXX, XXX, XXX−XXX

Here we have used the fact that $v(3, 4)$ is local in time, i.e., $v(3, 4) = v(\mathbf{r}_3 - \mathbf{r}_4)\delta(t_3 - t_4)$.

2. Plug the quasiparticle expression for the single-particle Green's function in the time domain

$$G_1(\mathbf{x}, \mathbf{x}', t - t') = -\frac{\mathrm{i}}{\hbar}\left[\sum_a \phi_a(\mathbf{x})\phi_a^*(\mathbf{x}')\theta(t - t')\mathrm{e}^{-\mathrm{i}\varepsilon_a^{\mathrm{QP}}(t-t')/\hbar} - \sum_i \phi_i(\mathbf{x})\phi_i^*(\mathbf{x}')\theta(t' - t)\mathrm{e}^{-\mathrm{i}\varepsilon_i^{\mathrm{QP}}(t-t')/\hbar}\right] \quad (36)$$

into eq 35, where $\varepsilon_s^{\mathrm{QP}}$ stands for the quasiparticle energy of orbital s. Here we assume that ϕ_i and ϕ_a (and $\mathbf{x}$ and $\mathbf{x}'$) have the same spin, i.e., $\sigma = \sigma'$. After plugging in, we multiply both sides of eq 33 by $\phi_a^*(\mathbf{x}_1)\phi_i(\mathbf{x}_{1'})$ and integrate over $\int\int \mathrm{d}\mathbf{x}_1\, \mathrm{d}\mathbf{x}_{1'}$. Setting $t_{1'} = t_1 + \delta(\delta \to 0^+)$, we find

$$\iint \mathrm{d}\mathbf{x}_1\, \mathrm{d}\mathbf{x}_{1'}\, \phi_i(\mathbf{x}_{1'})\phi_a^*(\mathbf{x}_1)\chi_S^{\mathrm{eh}}(\mathbf{x}_1, \mathbf{x}_{1'}; -\delta)\mathrm{e}^{-\mathrm{i}\Omega_S\tilde{t}_1/\hbar} = \iint \mathrm{d}\mathbf{x}_3\, \mathrm{d}\mathbf{x}_{3'}\, \frac{\phi_i(\mathbf{x}_3)\phi_a^*(\mathbf{x}_3)}{\Omega_S - \varepsilon_a^{\mathrm{QP}} + \varepsilon_i^{\mathrm{QP}}} v(\mathbf{r}_3 - \mathbf{r}_{3'})\chi_S^{\mathrm{eh}}(\mathbf{x}_{3'}, \mathbf{x}_{3'}; -\delta)\mathrm{e}^{-\mathrm{i}\Omega_S\tilde{t}_1/\hbar}$$
$$+ \iint \mathrm{d}\mathbf{x}_3\, \mathrm{d}\mathbf{x}_{3'}\, \frac{\phi_i(\mathbf{x}_{3'})\phi_a^*(\mathbf{x}_3)}{\Omega_S - \varepsilon_a^{\mathrm{QP}} + \varepsilon_i^{\mathrm{QP}}} \int_{-\infty}^{+\infty} \mathrm{d}\tau_3\, W(\mathbf{r}_3, \mathbf{r}_{3'}; \tau_3^+) \times (\theta(\tau_3)\mathrm{e}^{\mathrm{i}\tau_3(\varepsilon_i^{\mathrm{QP}} + (\Omega_S/2))/\hbar} + \theta(-\tau_3)\mathrm{e}^{\mathrm{i}\tau_3(\varepsilon_a^{\mathrm{QP}} - (\Omega_S/2))/\hbar})$$
$$\times \chi_S^{\mathrm{eh}}(\mathbf{x}_3, \mathbf{x}_{3'}; \tau_3)\mathrm{e}^{-\mathrm{i}\Omega_S\tilde{t}_1/\hbar} \quad (37)$$

To derive eq 37, we have performed a few integrations over time. On the right-hand side, in the first term, the only relevant terms require $t_1 > t_3 = t_{3'}$; in the second term, the only relevant terms are $t_1 > t_3$, $t_{3'}$. To tackle the second term, we change integration variables from t_3, $t_{3'}$ to τ_3, $\tilde{t}_3$, where

$$t_3 = \tilde{t}_3 + \frac{1}{2}\tau_3 \qquad t_{3'} = \tilde{t}_3 - \frac{1}{2}\tau_3$$

For the case $\tau_3 > 0$, the relevant terms satisfy $\tilde{t}_3 < t_1 - \frac{1}{2}\tau_3$; for the case $\tau_3 < 0$, the relevant terms satisfy $\tilde{t}_3 < t_1 + \frac{1}{2}\tau_3$.

3. Multiply both sides of eq 37 by $\Omega_S - \varepsilon_a^{\mathrm{QP}} + \varepsilon_i^{\mathrm{QP}}$ and drop the common factor $\mathrm{e}^{-\mathrm{i}\Omega_S\tilde{t}_1/\hbar}$. We find

$$(\Omega_S - \varepsilon_a^{\mathrm{QP}} + \varepsilon_i^{\mathrm{QP}})\iint \mathrm{d}\mathbf{x}_1\, \mathrm{d}\mathbf{x}_{1'}\, \phi_i(\mathbf{x}_{1'})\phi_a^*(\mathbf{x}_1)\chi_S^{\mathrm{eh}}(\mathbf{x}_1, \mathbf{x}_{1'}; -\delta) = \iint \mathrm{d}\mathbf{x}_3\, \mathrm{d}\mathbf{x}_{3'}\, \phi_i(\mathbf{x}_3)\phi_a^*(\mathbf{x}_3)v(\mathbf{r}_3 - \mathbf{r}_{3'})\chi_S^{\mathrm{eh}}(\mathbf{x}_{3'}, \mathbf{x}_{3'}; -\delta)$$
$$+ \iint \mathrm{d}\mathbf{x}_3\, \mathrm{d}\mathbf{x}_{3'}\, \phi_i(\mathbf{x}_{3'})\phi_a^*(\mathbf{x}_3)\int_{-\infty}^{+\infty} \mathrm{d}\tau_3\, W(\mathbf{r}_3, \mathbf{r}_{3'}; \tau_3^+) \times (\theta(\tau_3)\mathrm{e}^{\mathrm{i}\tau_3(\varepsilon_i^{\mathrm{QP}} + (\Omega_S/2))/\hbar} + \theta(-\tau_3)\mathrm{e}^{\mathrm{i}\tau_3(\varepsilon_a^{\mathrm{QP}} - (\Omega_S/2))/\hbar})\chi_S^{\mathrm{eh}}(\mathbf{x}_3, \mathbf{x}_{3'}; \tau_3) \quad (38)$$

4. Make the ansatz that $\chi_S^{\mathrm{eh}}(\mathbf{x}, \mathbf{x}'; \tau)$ can be expanded into an incomplete MO basis set that contains only the occupied−virtual and virtual−occupied parts with simple time dependence. This ansatz corresponds to Assumption #3 of the BSE approach

$$\chi_S^{\mathrm{eh}}(\mathbf{x}, \mathbf{x}'; \tau) = -\mathrm{e}^{\mathrm{i}\Omega_S|\tau|/2\hbar}\sum_{jb}\left[(\langle N|\hat{a}_j^\dagger\hat{a}_b|N_S\rangle\phi_b(\mathbf{x})\phi_j^*(\mathbf{x}') + \langle N|\hat{a}_b^\dagger\hat{a}_j|N_S\rangle\phi_j(\mathbf{x})\phi_b^*(\mathbf{x}'))\times(\theta(\tau)\mathrm{e}^{-\mathrm{i}\tau\varepsilon_b^{\mathrm{QP}}/\hbar} + \theta(-\tau)\mathrm{e}^{-\mathrm{i}\tau\varepsilon_j^{\mathrm{QP}}/\hbar})\right] \quad (39)$$
$$\equiv -\mathrm{e}^{\mathrm{i}\Omega_S|\tau|/2\hbar}\sum_{jb}\left[(\tilde{X}_{jb}^S\phi_b(\mathbf{x})\phi_j^*(\mathbf{x}') + \tilde{Y}_{jb}^S\phi_j(\mathbf{x})\phi_b^*(\mathbf{x}'))\times(\theta(\tau)\mathrm{e}^{-\mathrm{i}\tau\varepsilon_b^{\mathrm{QP}}/\hbar} + \theta(-\tau)\mathrm{e}^{-\mathrm{i}\tau\varepsilon_j^{\mathrm{QP}}/\hbar})\right] \quad (40)$$

where $\tilde{X}_{jb}^S$ and $\tilde{Y}_{jb}^S$ are defined as $\tilde{X}_{jb}^S \equiv \langle N|\hat{a}_j^\dagger\hat{a}_b|N_S\rangle$ and $\tilde{Y}_{jb}^S \equiv \langle N|\hat{a}_b^\dagger\hat{a}_j|N_S\rangle$.

5. By definition, ϕ_i and ϕ_a have the same spin in eq 38, i.e., $\mathbf{x}_1$ and $\mathbf{x}_{1'}$ have the same spin on the left-hand side of eq 38 (inside of the integral). Now, we plug eq 40 into eq 38 and Fourier transform the screened potential $W(\tau) = \frac{1}{2\pi}\int_{-\infty}^{\infty}\mathrm{d}\omega\, \mathrm{e}^{-\mathrm{i}\omega t}W(\omega)$. Next, we perform the integral over τ_3 and add an infinitesimal imaginary amplitude $\mathrm{e}^{-\mathrm{i}\eta|\tau_3|}$ with $\eta > 0$ to force the integration over τ_3 to converge. Repeat the exact same analysis for $\tilde{\chi}_S^{\mathrm{eh}}(\mathbf{x}, \mathbf{x}'; \tau)$. The generalized eigenvalue problem for BSE finally reads

$$\begin{pmatrix} \tilde{\mathbf{A}}^S & \tilde{\mathbf{B}}^S \\ -\tilde{\mathbf{B}}^S & -\tilde{\mathbf{A}}^S \end{pmatrix}\begin{pmatrix} \tilde{\mathbf{X}}^S \\ \tilde{\mathbf{Y}}^S \end{pmatrix} = \Omega_S\begin{pmatrix} \tilde{\mathbf{X}}^S \\ \tilde{\mathbf{Y}}^S \end{pmatrix} \quad (41)$$

for electron−hole excitation amplitudes $\tilde{\mathbf{X}}^S$ and $\tilde{\mathbf{Y}}^S$ and excitation energy Ω_S for BSE excited state S. $\tilde{\mathbf{A}}^S$ and $\tilde{\mathbf{B}}^S$ have the following matrix elements

$$\tilde{A}_{iajb}^S = \delta_{ij}\delta_{ab}(\varepsilon_a^{\mathrm{QP}} - \varepsilon_i^{\mathrm{QP}}) + K_{iajb}^S \quad (42)$$

$$\tilde{B}_{iajb}^S = K_{iabj}^S \quad (43)$$

where

$$K_{iabj}^S = K_{iabj}^x + K_{iabj}^d(\Omega_S) \quad (44)$$

$$K_{iajb}^x = \iint \mathrm{d}\mathbf{r}\, \mathrm{d}\mathbf{r}'\, \phi_i(\mathbf{r})\phi_a(\mathbf{r})\phi_j(\mathbf{r}')\phi_b(\mathbf{r}')v(\mathbf{r}, \mathbf{r}') \quad (45)$$
$$= (ia|jb) \quad (46)$$

DOI: 10.1021/acs.jctc.7b00246
J. Chem. Theory Comput. XXXX, XXX, XXX−XXX

$$K^{d}_{iajb}(\Omega_S) = -\iint \mathrm{d}\mathbf{r}\,\mathrm{d}\mathbf{r}'\;\phi_a(\mathbf{r})\phi_b(\mathbf{r})\phi_i(\mathbf{r}')\phi_j(\mathbf{r}') \times \frac{\mathrm{i}}{2\pi}\int \mathrm{d}\omega\; \mathrm{e}^{-\mathrm{i}\omega\eta} W(\mathbf{r}, \mathbf{r}', \omega) \times \left[\frac{1}{\Omega_S - \hbar\omega - (\varepsilon_b^{\mathrm{QP}} - \varepsilon_i^{\mathrm{QP}}) + \mathrm{i}\eta} + \frac{1}{\Omega_S + \hbar\omega - (\varepsilon_a^{\mathrm{QP}} - \varepsilon_j^{\mathrm{QP}}) + \mathrm{i}\eta}\right] \tag{47}$$

In eqs 45 and 46, ϕ_i, ϕ_a, ϕ_j, and ϕ_b are spin orbitals that we have assumed to be real valued. Furthermore, in eq 45, we require only that $\sigma_i = \sigma_a$ and $\sigma_j = \sigma_b$ such that same spin and opposite spin cases are allowed; in eq 47, we require complete spin alignment, $\sigma_i = \sigma_a = \sigma_j = \sigma_b$. The factor $\mathrm{e}^{-\mathrm{i}\omega\eta}$ is included in eq 47 to remind us only that, if we seek to evaluate the integral over a complex, that contour must run below the real axis.

2.A.3. Quasiparticle Energies from the GW Approximation. To evaluate eq 47 in practice, we require a *GW* calculation on top of a Hartree calculation to extract the quasiparticle energy.[40] To avoid a self-consistent calculation, the standard approach is to apply a linear expansion for the real part of the correlation part of the self-energy $\Sigma^c(\omega)$

$$\mathrm{Re}\,\Sigma^c(\varepsilon_s^{GW}) \approx \mathrm{Re}\,\Sigma^c(\varepsilon_s^{\mathrm{H}}) + \frac{\varepsilon_s^{GW} - \varepsilon_s^{\mathrm{H}}}{\hbar}\frac{\partial\,\mathrm{Re}\,\Sigma^c(\varepsilon_s^{\mathrm{H}})}{\partial\omega} \tag{48}$$

which leads to

$$\varepsilon_s^{GW} \approx \varepsilon_s^{\mathrm{H}} + Z_s\,\mathrm{Re}\,\Sigma^c(\varepsilon_s^{\mathrm{H}}) + \Sigma_s^x \tag{49}$$

where $\varepsilon_s^{\mathrm{H}}$ denotes the Hartree orbital energy and ε_s^{GW} denotes the *GW* orbital energy. The quasiparticle renormalization factor Z_s is given by

$$Z_s \equiv \left(1 - \frac{\partial\,\mathrm{Re}\,\Sigma^c(\varepsilon_s^{\mathrm{H}})}{\partial\omega}\right)^{-1} \tag{50}$$

In ref 40, for a finite Hubbard model, we found that the *Z*-factor values for orbitals other than the HOMO and LUMO were usually far from unity with correspondingly large errors compared to exact attachment−detachment energies. As a result, in this work, we calculate $Z_s\,\mathrm{Re}\,\Sigma^c(\varepsilon_s^{\mathrm{H}})$ for only the HOMO and LUMO. After adding in the exchange part of the self-energy Σ_s^x, we shift all of the virtual (occupied) orbitals by $Z_{\mathrm{lumo}}\,\mathrm{Re}\,\Sigma^c(\varepsilon_{\mathrm{lumo}}^{\mathrm{H}})$ ($Z_{\mathrm{homo}}\,\mathrm{Re}\,\Sigma^c(\varepsilon_{\mathrm{homo}}^{\mathrm{H}})$), i.e.

$$\varepsilon_a^{GW} \approx \varepsilon_a^{\mathrm{H}} + Z_{\mathrm{lumo}}\,\mathrm{Re}\,\Sigma^c(\varepsilon_{\mathrm{lumo}}^{\mathrm{H}}) + \Sigma_a^x \tag{51}$$

$$\varepsilon_i^{GW} \approx \varepsilon_i^{\mathrm{H}} + Z_{\mathrm{homo}}\,\mathrm{Re}\,\Sigma^c(\varepsilon_{\mathrm{homo}}^{\mathrm{H}}) + \Sigma_i^x \tag{52}$$

2.A.4. Matrix Elements for the Electron−Hole Interacting Kernel. After the approximate quasiparticle energy ε_p^{GW} is obtained, the next step is to build the electron−hole interaction kernel *K*. The matrix elements of K^x(35, 46) (in the MO basis) are simply given by eq 46. In order to obtain the matrix elements of K^d, we recall the expression for the screened Coulomb interaction *W*[40,44,45]

$$W(\mathbf{r}, \mathbf{r}'; \omega) = v(\mathbf{r}, \mathbf{r}') + \int \mathrm{d}\mathbf{r}''\,\mathrm{d}\mathbf{r}'''\; v(\mathbf{r}, \mathbf{r}'')\chi(\mathbf{r}'', \mathbf{r}''', \omega)v(\mathbf{r}''', \mathbf{r}') \tag{53}$$

$$\equiv v(\mathbf{r}, \mathbf{r}') + W^p(\mathbf{r}, \mathbf{r}'; \omega) \tag{54}$$

where $W^p(\mathbf{r}, \mathbf{r}'; \omega)$ is defined as

$$W^p(\mathbf{r}, \mathbf{r}'; \omega) \equiv \int \mathrm{d}\mathbf{r}''\,\mathrm{d}\mathbf{r}'''\; v(\mathbf{r}, \mathbf{r}'')\chi(\mathbf{r}'', \mathbf{r}''', \omega)v(\mathbf{r}''', \mathbf{r}') \tag{55}$$

Here $\chi(\mathbf{r}'', \mathbf{r}''', \omega)$ is the time-dependent Hartree (TDH) polarizability in the frequency domain and is computed via the following sum-over-states expression[46] in a MO basis

$$\chi(\omega) = \left[\begin{pmatrix}\mathbf{A} & \mathbf{B}\\ \mathbf{B} & \mathbf{A}\end{pmatrix} + \omega\begin{pmatrix}\mathbf{I} & 0\\ 0 & -\mathbf{I}\end{pmatrix}\right]^{-1} \tag{56}$$

$$= \sum_I \left[\frac{1}{\Omega_I^{\mathrm{TDH}} + \hbar\omega}\begin{pmatrix}\mathbf{X}^I\\ \mathbf{Y}^I\end{pmatrix}(\mathbf{X}^I \quad \mathbf{Y}^I) + \frac{1}{\Omega_I^{\mathrm{TDH}} - \hbar\omega}\begin{pmatrix}\mathbf{Y}^I\\ \mathbf{X}^I\end{pmatrix}(\mathbf{Y}^I \quad \mathbf{X}^I)\right] \tag{57}$$

where $\mathbf{X}^I$ and $\mathbf{Y}^I$ correspond to the TDH excitation amplitudes of excited state *I* with excitation energy Ω_I^{TDH}.

In terms of MOs, if the perturbing potential is independent of spin and of the form $u_{jb}(t)(a_b^\dagger a_j + a_j^\dagger a_b)$, one finds that the response function is

$$\chi_{iajb}(\omega) = \sum_I \left[\frac{M^I_{iajb}}{\Omega_I^{\mathrm{TDH}} + \hbar\omega - \mathrm{i}\eta} + \frac{M^I_{iajb}}{\Omega_I^{\mathrm{TDH}} - \hbar\omega - \mathrm{i}\eta}\right] \tag{58}$$

where

$$M^I_{iajb} = X^I_{ia}X^I_{jb} + X^I_{ia}Y^I_{jb} + Y^I_{ia}X^I_{jb} + Y^I_{ia}Y^I_{jb} \tag{59}$$

In real space

$$\chi(\mathbf{r}, \mathbf{r}', \omega) = \sum_I \sum_{iajb} \phi_i(\mathbf{r})\phi_a(\mathbf{r})\phi_j(\mathbf{r}')\phi_b(\mathbf{r}') \times \left[\frac{M^I_{iajb}}{\Omega_I^{\mathrm{TDH}} + \hbar\omega - \mathrm{i}\eta} + \frac{M^I_{iajb}}{\Omega_I^{\mathrm{TDH}} - \hbar\omega - \mathrm{i}\eta}\right] \tag{60}$$

For this paper, we assume that the ground state of the system is a closed-shell singlet so that all up-spin and down-spin orbitals have the same spatial components. Thus, in eq 60, one can sum over the spin components and produce a spatial $\tilde{M}_I$ matrix

$$\tilde{M}^I_{iajb} = \sum_{\sigma_i=\sigma_a,\sigma_j=\sigma_b} M^I_{iajb} \tag{61}$$

We can then rewrite eq 60 as follows

DOI: 10.1021/acs.jctc.7b00246
J. Chem. Theory Comput. XXXX, XXX, XXX−XXX

$$\chi(\mathbf{r}, \mathbf{r}', \omega) = \sum_I{}' \sum_{iajb} \phi_i(\mathbf{r})\phi_a(\mathbf{r})\phi_j(\mathbf{r}')\phi_b(\mathbf{r}') \times \left[\frac{\tilde{M}^I_{iajb}}{\Omega_I^{\mathrm{TDH}} + \hbar\omega - \mathrm{i}\eta} + \frac{\tilde{M}^I_{iajb}}{\Omega_I^{\mathrm{TDH}} - \hbar\omega - \mathrm{i}\eta} \right] \tag{62}$$

where $\sum'$ denotes a sum over only spatial orbitals. Note that only singlet states contribute to the sum-over-states in eq 62; all triplet contributions cancel exactly.

Finally, using eq 55, the matrix elements for W^p in real space are

$$W^p(\mathbf{r}, \mathbf{r}', \omega) = \sum_I \sum_{iajb}{}' \phi_i(\mathbf{r})\phi_a(\mathbf{r})\phi_j(\mathbf{r}')\phi_b(\mathbf{r}') \times \sum_{kcld}{}' (ia|kc)(jb|ld) \left[\frac{\tilde{M}^I_{kcld}}{\Omega_I^{\mathrm{TDH}} + \hbar\omega - \mathrm{i}\eta} + \frac{\tilde{M}^I_{kcld}}{\Omega_I^{\mathrm{TDH}} - \hbar\omega - \mathrm{i}\eta} \right] \tag{63}$$

The matrix elements in a spatial MO basis are

$$W^p_{iajb} = \sum_I \sum_{kcld}{}' (ia|kc)(jb|ld) \left[\frac{\tilde{M}^I_{kcld}}{\Omega_I^{\mathrm{TDH}} + \hbar\omega - \mathrm{i}\eta} + \frac{\tilde{M}^I_{kcld}}{\Omega_I^{\mathrm{TDH}} - \hbar\omega - \mathrm{i}\eta} \right] \tag{64}$$

and the matrix elements in an AO basis are

$$W^p_{\mu\nu\lambda\sigma} = \sum_{iajb}{}' C_{\mu a} C_{\lambda b} C_{\nu i} C_{\sigma j} W^p_{iajb} \tag{65}$$

Equation 47 is now ready to be evaluated with the help of eqs 54, 64, and 65. Obviously, if one neglects the polarizable part of the screened Coulomb interaction W^p in eqs 54, one will recover TDHF exactly from BSE (eqs 41−43).

2.A.5. Frequency-Independent Electron−Hole Interaction Kernel. In many cases (e.g., in most semiconductor crystals), the excitations in state $|\Psi_S\rangle$ are mainly composed of electron−hole pair configurations $|\Phi_i^a\rangle$ whose transition energies $(\varepsilon_a^{\mathrm{QP}} - \varepsilon_i^{\mathrm{QP}})$ are close to the resulting excitation energy Ω_S, which means that $\Omega_S - (\varepsilon_a^{\mathrm{QP}} - \varepsilon_i^{\mathrm{QP}})$ is much smaller than Ω_I^{TDH}.[35] In such cases, eq 47 can be approximated by

$$K^d_{iajb} = -\int \mathrm{d}\mathbf{r}\, \mathrm{d}\mathbf{r}'\, \phi_i(\mathbf{r})\phi_a(\mathbf{r}')\phi_j(\mathbf{r})\phi_b(\mathbf{r}') \times W^p(\mathbf{r}, \mathbf{r}', \omega = 0) \tag{66}$$

$$= -\sum_{\mu\nu\lambda\sigma}{}' C_{\mu a} C_{\lambda b} C_{\nu i} C_{\sigma_j} W^p_{\mu\nu\lambda\sigma}(\omega = 0) \tag{67}$$

where

$$W^p_{\mu\nu\lambda\sigma}(\omega = 0) = \sum_{iajb}{}' C_{\mu a} C_{\lambda b} C_{\nu i} C_{\sigma j} \sum_I \sum_{kcld}{}' (ia|kc)(jb|ld) \times \left[\frac{\tilde{M}^I_{kcld}}{\Omega_I^{\mathrm{TDH}} - \mathrm{i}\eta} + \frac{\tilde{M}^I_{kcld}}{\Omega_I^{\mathrm{TDH}} - \mathrm{i}\eta} \right] \tag{68}$$

2.A.6. Summary. The derivation of BSE (eqs 41−43) reviewed above is summarized in Figure 2. BSE can be solved either directly (without further approximation, i.e., the random phase approximation (RPA)) or within the Tamm−Dancoff approximation (TDA), which sets the matrix $\mathbf{B} = 0$. In this work, we will test both versions. We also will study the self-consistent

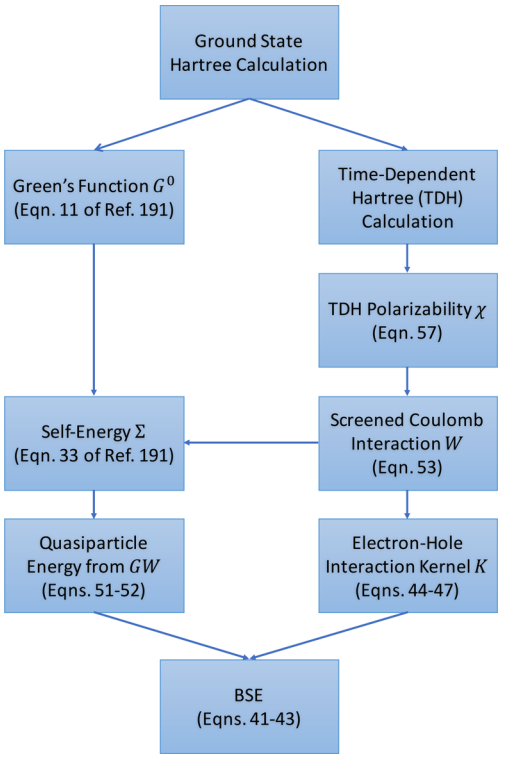

Figure 2. Flowchart for how to calculate BSE energies in practice.

(using eq 47 for K^d) and the non-self-consistent (using eq 66 for K^d) versions of BSE. This completes our (tedious but comprehensive) derivation of the BSE approach.

2.B. Configuration Interaction Approaches. Our goal in this paper is to compare BSE with CI approaches. For completeness, we now review the relevant quantum chemistry approaches.

2.B.1. CIS/TDHF. The simplest CI method, CIS, includes only the single-excitation manifold. The matrix elements of the CIS Hamiltonian are

$$A^{\mathrm{CIS}}_{iajb} = \langle \Phi_i^a | \hat{H} | \Phi_j^b \rangle = \delta_{ij}\delta_{ab}(\varepsilon_a - \varepsilon_i) + \langle aj||ib\rangle \tag{69}$$

where $\langle aj||ib\rangle \equiv \langle aj|ib\rangle - \langle aj|bi\rangle$ is the two-electron integral. The CIS wave function can be written as

$$|\Psi_I^{\mathrm{CIS}}\rangle = \sum_{ia} t_i^{Ia} |\Phi_i^a\rangle \tag{70}$$

where t_i^{Ia} is the excitation coefficients for CIS excited state I. With low computational cost, CIS is applicable to very large systems. However, in general, CIS only gives qualitatively correct results.

The same qualitative features apply equally to TDHF, which is a slight generalization of CIS. According to TDHF, which is a response theory based on top of a HF (not Hartree) ground state, the excitation energies are computed by diagonalizing

$$\begin{pmatrix} \mathbf{A}^{\mathrm{TDHF}} & \mathbf{B}^{\mathrm{TDHF}} \\ -\mathbf{B}^{\mathrm{TDHF}} & -\mathbf{A}^{\mathrm{TDHF}} \end{pmatrix} \tag{71}$$

where $A^{\mathrm{TDHF}}_{iajb} = A^{\mathrm{CIS}}_{iajb}$ and $B^{\mathrm{TDHF}}_{iajb} = \langle ab||ij\rangle$. Like CIS, TDHF is usually not accurate quantitatively.[47]

2.B.2. CIS(D). CIS(D) serves as a nondegenerate perturbative second-order correction to CIS that approximately introduces effects of electron correlation and double-excitations for the excited states in a noniterative scheme.[22] In CIS(D), MP2 theory

DOI: 10.1021/acs.jctc.7b00246
J. Chem. Theory Comput. XXXX, XXX, XXX−XXX

is employed in order to include electron correlation in the ground state. The original unperturbed Hamiltonian $\hat{H}_0$ is chosen as the Fock operator. Then, with perturbation V, the total Hamiltonian becomes

$$\hat{H} = \hat{H}_0 + \lambda\hat{V} \tag{72}$$

and performing second-order time-independent perturbation theory, one recovers the MP2 correction to the ground-state energy

$$\omega_0^{\mathrm{MP2}} = \langle\Phi_0|\hat{V}\hat{T}_2|\Phi_0\rangle \tag{73}$$

$$= -\frac{1}{4}\sum_{ijab}\frac{|\langle\Phi_0|\hat{V}|\Phi_{ij}^{ab}\rangle|^2}{\varepsilon_a + \varepsilon_b - \varepsilon_i - \varepsilon_j} \tag{74}$$

$$= -\frac{1}{4}\sum_{ijab}\frac{|\langle ij||ab\rangle|^2}{\varepsilon_a + \varepsilon_b - \varepsilon_i - \varepsilon_j} \tag{75}$$

where $\hat{T}_2$ is the double-excitation operator that yields the double-excitation manifold $|\Phi_{ij}^{ab}\rangle$ with the effective excitation coefficients

$$\hat{T}_2 = \frac{1}{4}\sum_{ijab} d_{ij}^{ab}\hat{a}_a^\dagger\hat{a}_b^\dagger\hat{a}_i\hat{a}_j \tag{76}$$

$$d_{ij}^{ab} \equiv -\sum_{ijab}\frac{\langle\Phi_0|\hat{V}|\Phi_{ij}^{ab}\rangle}{\varepsilon_a + \varepsilon_b - \varepsilon_i - \varepsilon_j} \tag{77}$$

$$= -\sum_{ijab}\frac{\langle ij||ab\rangle}{\varepsilon_a + \varepsilon_b - \varepsilon_i - \varepsilon_j} \tag{78}$$

Note that the single-excitation manifold does not appear in the MP2 energy because of Brillouin's theorem.

Now, CIS(D) is consistent with MP2 theory performed on CIS excited states and includes the corrections to the CIS excitation energy from three sources: single- and double-excitations with respect to the CIS wave function and again the MP2 correction to the ground-state energy. Therefore, we may write

$$\omega_I^{\mathrm{CIS(D)}} = \langle\Psi_I^{\mathrm{CIS}}|\hat{V}\hat{T}_1|\Psi_I^{\mathrm{CIS}}\rangle + \langle\Psi_I^{\mathrm{CIS}}|\hat{V}\hat{T}_2|\Psi_I^{\mathrm{CIS}}\rangle - \omega_0^{\mathrm{MP2}} \tag{79}$$

Overall, the single-excitation operator acting on the CIS state in the first term gives an overall double-excitation

$$\hat{T}_1 \equiv -\frac{1}{4}\sum_{ijab}\frac{|\Phi_{ij}^{ab}\rangle\langle\Phi_{ij}^{ab}|}{\varepsilon_a + \varepsilon_b - \varepsilon_i - \varepsilon_j - \Omega_I^{\mathrm{CIS}}}\hat{V} \tag{80}$$

Plugging eq 80 into eq 79, one finds that the first term in eq 79 finally yields

$$\langle\Psi_I^{\mathrm{CIS}}|\hat{V}\hat{T}_1|\Psi_I^{\mathrm{CIS}}\rangle = -\frac{1}{4}\sum_{ijab}\frac{(s_{ij}^{ab})^2}{\varepsilon_a + \varepsilon_b - \varepsilon_i - \varepsilon_j - \Omega_I^{\mathrm{CIS}}} \tag{81}$$

$$s_{ij}^{ab} \equiv \langle\Psi_I^{\mathrm{CIS}}|\hat{V}|\Phi_{ij}^{ab}\rangle \tag{82}$$

$$= \sum_{kc} t_k^{Ic}\langle\Phi_k^c|\hat{V}|\Phi_{ij}^{ab}\rangle \tag{83}$$

$$= \sum_{c}[\langle ab||cj\rangle t_i^{Ic} - \langle ab||ci\rangle t_j^{Ic}] + \sum_{k}[\langle ka||ij\rangle t_k^{Ib} - \langle kb||ij\rangle t_k^{Ia}] \tag{84}$$

The second term in eq 79 gives a triple-excitation with respect to the ground state. Note that in CIS(D), the double-excitation operator that acts on CIS excited states $\hat{T}_2$ remains the same as the operator acting on the ground state in MP2 theory, i.e., the corresponding excitation coefficients d_{ij}^{ab} are not changed. Therefore, the second term in eq 79 finally yields

$$\langle\Psi_I^{\mathrm{CIS}}|\hat{V}\hat{T}_2|\Psi_I^{\mathrm{CIS}}\rangle = \sum_{klcd} t_k^{Ic}t_l^{Id}\langle\Phi_k^c|\hat{V}\hat{T}_2|\Phi_l^d\rangle \tag{85}$$

$$= \langle\Phi_0|\hat{V}\hat{T}_2|\Phi_0\rangle + 2\sum_{ia} t_i^{Ia}\sum_{klcd}\langle kl||cd\rangle(t_i^{Ic}d_{kl}^{da} + t_k^{Ia}d_{il}^{dc} + 2t_k^{Ic}d_{il}^{ad}) \tag{86}$$

$$= \omega_0^{\mathrm{MP2}} + \frac{1}{2}\sum_{ia} t_i^{Ia}\sum_{klcd}\langle kl||cd\rangle(t_i^{Ic}d_{kl}^{da} + t_k^{Ia}d_{il}^{dc} + 2t_k^{Ic}d_{il}^{ad}) \tag{87}$$

Note that the MP2 correction energy cancels within CIS(D) and the final CIS(D) correction for CIS state I can be represented as

$$\omega_I^{\mathrm{CIS(D)}} = -\frac{1}{4}\sum_{ijab}\frac{(s_{ij}^{ab})^2}{\varepsilon_a + \varepsilon_b - \varepsilon_i - \varepsilon_j - \Omega_I^{\mathrm{CIS}}} + \frac{1}{2}\sum_{ia} t_i^{Ia}\sum_{klcd}\langle kl||cd\rangle(t_i^{Ic}d_{kl}^{da} + t_k^{Ia}d_{il}^{dc} + 2t_k^{Ic}d_{il}^{ad}) \tag{88}$$

CIS(D) is a second-order nondegenerate perturbation method on top of CIS and requires no extra diagonalization beyond the CIS Hamiltonian.

2.B.3. CIS(D$_n$). To generalize CIS(D) to the near-degenerate case, there is a well-known family of quasi-degenerate second-order perturbation theories known as CIS(D$_n$).[28] Within CIS(D$_n$), one diagonalizes a perturbed Hamiltonian that contains only single- and double-excitations to second order

$$H^{\mathrm{CIS(D}_n)} = \begin{pmatrix} H_{SS}^{(0)} + H_{SS}^{(2)} & H_{SD}^{(1)} \\ (H_{SD}^{(1)})^\dagger & H_{DD}^{(0)} \end{pmatrix} \tag{89}$$

where

$$(H_{SS}^{(0)})_{iajb} = \langle\Phi_i^a|\hat{H}_0|\Phi_j^b\rangle \tag{90}$$

$$(H_{SS}^{(2)})_{iajb} = \langle\Phi_i^a|\hat{V}\hat{T}_2|\Phi_j^b\rangle \tag{91}$$

DOI: 10.1021/acs.jctc.7b00246
J. Chem. Theory Comput. XXXX, XXX, XXX−XXX

$$(H^{(1)}_{SD})_{ia,jbkc} = \langle \Phi^a_i | \hat{V} | \Phi^{bc}_{jk} \rangle \tag{92}$$

$$(H^{(0)}_{DD})_{iajb,kcld} = \langle \Phi^{ab}_{ij} | \hat{F} | \Phi^{cd}_{kl} \rangle \tag{93}$$

Note that the ground-state response is taken into consideration through the $H^{(2)}_{SS}$ sub-block by including the double-excitation operator $\hat{T}_2$ from ground-state MP2 theory. Note also that a zeroth-order approximation is applied to the $H^{(0)}_{DD}$ sub-block so that only the diagonal elements appear in this sub-block. Thus, the $H^{(0)}_{DD}$ block can be formally inverted, leading to a much smaller, energy-dependent Hamiltonian matrix (and a corresponding self-consistent energy-dependent eigenvalue equation)

$$\mathcal{H}^{\mathrm{CIS(D}_n\mathrm{)}}(\omega) = H^{(0)}_{SS} + H^{(2)}_{SS} - H^{(1)}_{SD}(H^{(0)}_{DD} - \omega)^{-1}(H^{(1)}_{SD})^{\dagger} \tag{94}$$

Note that $(H^{(0)}_{DD} - \omega)^{-1}$ can be written as an expansion

$$(H^{(0)}_{DD} - \omega)^{-1} = (H^{(0)}_{DD})^{-1}(\mathbf{1} - \Delta)^{-1} \tag{95}$$

$$= (H^{(0)}_{DD})^{-1}(\mathbf{1} + \Delta + \Delta^2 + \cdots) \tag{96}$$

where Δ*is* defined as

$$\Delta \equiv \omega(H^{(0)}_{DD})^{-1} \tag{97}$$

The CIS(D_n) hierarchy at level n is defined as the method that results from truncating the expansion after the Δ^n term. As a result, the eigenvalue problem for CIS(D_0) simply becomes

$$(H^{(0)}_{SS} + H^{(2)}_{SS} - H^{(1)}_{SD}(H^{(0)}_{DD})^{-1}(H^{(1)}_{SD})^{\dagger})|\Psi^{\mathrm{CIS(D}_0\mathrm{)}}_I\rangle = \Omega^{\mathrm{CIS(D}_0\mathrm{)}}_I |\Psi^{\mathrm{CIS(D}_0\mathrm{)}}_I\rangle \tag{98}$$

where we define the CIS(D_0) Hamiltonian $\mathcal{H}^{\mathrm{CIS(D}_0\mathrm{)}}$ as

$$\mathcal{H}^{\mathrm{CIS(D}_0\mathrm{)}} \equiv H^{(0)}_{SS} + H^{(2)}_{SS} - H^{(1)}_{SD}(H^{(0)}_{DD})^{-1}(H^{(1)}_{SD})^{\dagger} \tag{99}$$

$$\mathcal{H}^{\mathrm{CIS(D}_0\mathrm{)}}_{iajb} = \delta_{ij}\delta_{ab}(\varepsilon_a - \varepsilon_i) + \langle ja||bi\rangle + \frac{1}{2}\sum_{kc}\langle jk||bc\rangle(\delta_{ij}d^{ca}_{jk} + \delta_{ab}d^{cb}_{ik} + 2d^{ac}_{ik}) - \frac{1}{2}\Big[\sum_{cdl}\langle ja||bc\rangle b^{bcd}_{ijl} + \sum_{dkl}\langle jk||ib\rangle b^{abd}_{jkl}\Big] \tag{100}$$

where d^{cb}_{ik} is defined in eqs 77 and 78 and b^{abc}_{ijk} is defined as

$$b^{abc}_{ijk} \equiv \frac{\langle ab||ci\rangle\delta_{jk} - \langle ab||cj\rangle\delta_{ik} + \langle kb||ij\rangle\delta_{ac} - \langle ka||ij\rangle\delta_{bc}}{\varepsilon_a + \varepsilon_b - \varepsilon_i - \varepsilon_j} \tag{101}$$

The effective CIS(D_1) Hamiltonian $\mathcal{H}^{\mathrm{CIS(D}_1\mathrm{)}}$ is defined as

$$\mathcal{H}^{\mathrm{CIS(D}_1\mathrm{)}} \equiv \mathcal{S}^{-1/2}\mathcal{H}^{\mathrm{CIS(D}_0\mathrm{)}}\mathcal{S}^{-1/2} \tag{102}$$

where

$$\mathcal{S} \equiv \mathbf{1} + H^{(1)}_{SD}(H^{(0)}_{DD})^{-2}(H^{(1)}_{SD})^{\dagger} \tag{103}$$

$$\mathcal{S}_{iajb} = \mathbf{1} + \frac{\sum_{cdl}\langle ja||bc\rangle b^{bcd}_{ijl} + \sum_{dkl}\langle jk||ib\rangle b^{abd}_{jkl}}{2(\varepsilon_a + \varepsilon_b - \varepsilon_i - \varepsilon_j)} \tag{104}$$

Finally, the full CIS(D_n) Hamiltonian given by eq 94 (without truncating $(H^{(0)}_{DD} - \omega)^{-1}$) corresponds to the CIS(D_∞) Hamiltonian. Solving the resulting energy-dependent eigenvalue equation of the CIS(D_∞) Hamiltonian (eq 105) self-consistently gives the CIS(D_∞) excitation energies

$$\mathcal{H}^{\mathrm{CIS(D}_\infty\mathrm{)}}(\omega)|\Psi^{\mathrm{CIS(D}_\infty\mathrm{)}}_I\rangle = \omega|\Psi^{\mathrm{CIS(D}_\infty\mathrm{)}}_I\rangle \tag{105}$$

2.B.4. Relation between CIS(D_n) and CC2 and ADC(2). Although in this paper we will focus exclusively on the CIS(D_n) suite of excited states, it is important to recall that the CIS(D_∞) Hamiltonian is nearly identical to several other excited-state Hamiltonians that are common in the literature.[24−27,48] Among them, the CC2 model, which is also know as the approximate coupled-cluster singles and doubles model, iteratively determines the singles and doubles substitutions as the poles of a true linear response function.[24,25,48]

Let us now remind the reader briefly of a few relevant details pertaining to CC2. In standard second-order coupled-cluster theory (CCSD) for the electronic ground state,[49] one performs a similarity transformation to the unperturbed Hamiltonian such that

$$\tilde{H} = \mathrm{e}^{-(\hat{T}^{\mathrm{CC}}_1 + \hat{T}^{\mathrm{CC}}_2)}\hat{H}\mathrm{e}^{(\hat{T}^{\mathrm{CC}}_1 + \hat{T}^{\mathrm{CC}}_2)} \tag{106}$$

where $\hat{T}^{\mathrm{CC}}_1$ and T^{CC}_2 are first- and second-order coupled-cluster operators

$$\hat{T}^{\mathrm{CC}}_1 = \sum_{ia} t^{\mathrm{CC}}_{ia}\hat{a}^{\dagger}_a\hat{a}_i \tag{107}$$

$$\hat{T}^{\mathrm{CC}}_2 = \sum_{ijab} t^{\mathrm{CC}}_{ijab}\hat{a}^{\dagger}_a\hat{a}^{\dagger}_b\hat{a}_i\hat{a}_j \tag{108}$$

The corresponding coefficients t^{CC}_{ia} and t^{CC}_{ijab} are determined via the CCSD amplitude equations

$$\sum_{ia} t^{\mathrm{CC}}_{ia}\langle \Phi^a_i|\tilde{H}|\Phi_{\mathrm{HF}}\rangle = 0 \tag{109}$$

$$\sum_{ijab} t^{\mathrm{CC}}_{ijab}\langle \Phi^{ab}_{ij}|\tilde{H}|\Phi_{\mathrm{HF}}\rangle = 0 \tag{110}$$

In CC2, the similarity transformation is approximated by

$$\mathrm{e}^{(\hat{T}^{\mathrm{CC}}_1 + \hat{T}^{\mathrm{CC}}_2)} \approx \mathrm{e}^{\hat{T}^{\mathrm{CC}}_1}(1 + \hat{T}^{\mathrm{CC}}_2) \tag{111}$$

and then one determines a ground-state CC2 energy and wave function in the same spirit as a CCSD calculation. Now, to determine excited-state energies, with CC2, a standard equation-of-motion calculation is performed on top of the CC2 ground state.[S0]

With this background in mind, we remind the reader that, as shown by Hättig,[48] the only essential difference between CC2 and CIS(D_∞) is that the double-excitation amplitudes are solved via ground-state MP2 theory in CIS(D_∞), while they are solved via approximated coupled-cluster theory as the ground-state cluster amplitudes in CC2

$$\mathcal{H}^{\mathrm{CC2}}(\omega) = H^{(0)}_{SS} + \tilde{H}^{(2)}_{SS} - H^{(1)}_{SD}(H^{(0)}_{DD} - \omega)^{-1}(H^{(1)}_{SD})^{\dagger} \tag{112}$$

$$(\tilde{H}^{(2)}_{SS})_{iajb} = \langle \Phi^a_i|\hat{V}\hat{T}^{\mathrm{CC}}_2|\Phi^b_j\rangle \tag{113}$$

Similarly, the model of algebraic diagrammatic construction through second order (ADC(2)) is effectively the symmetric or the Hermitian part of the CIS(D_∞) model. More precisely, note that $H^{(2)}_{SS}$ in eq 94 gives rise to a nonsymmetric form for the CIS(D_∞) Hamiltonian. The ADC(2) Hamiltonian is just the symmetrized form of the CIS(D_∞) Hamiltonian[26,27,48]

DOI: 10.1021/acs.jctc.7b00246
J. Chem. Theory Comput. XXXX, XXX, XXX−XXX

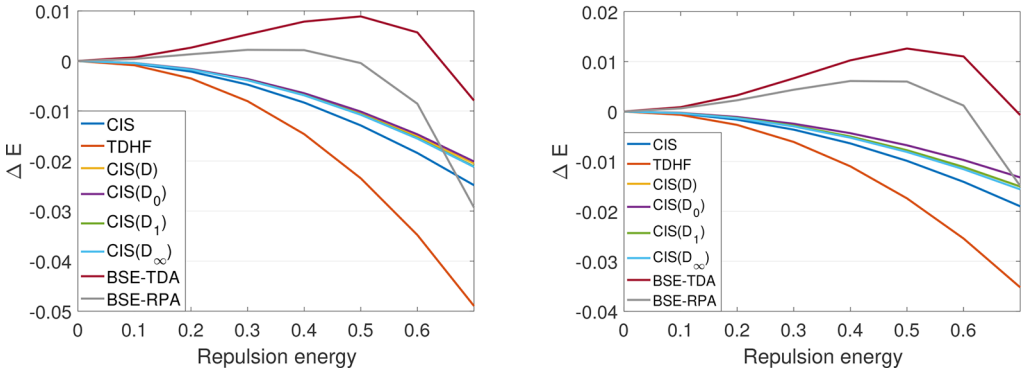

Figure 3. Errors for the excitation energy of the first (left, S_1) and second (right, S_2) excited singlet states for the metallic system ($V_\mu = 0$ for all sites μ, $\tau = 1.0$). All errors are relative to the exact diagonalization. None of these methods gives perfect results. All of the CI methods underestimate the energy while the BSE-TDA method generally overestimates the energy (except for $U = 0.7$). BSE-RPA is accurate for small Us but underestimates the energy for large Us.

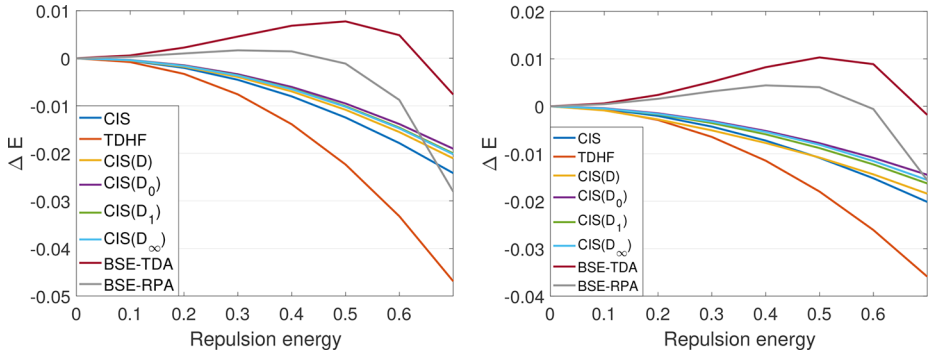

Figure 4. Errors for the excitation energy of the first (left, S_1) and second (right, S_2) excited singlet states for the doped system (with $V_5 = -0.5$). All errors are relative to the exact diagonalization. Results in this doped system are very similar to those in the metallic system.

$$\mathcal{H}^{\mathrm{ADC(2)}}(\omega) = \frac{1}{2}((\mathcal{H}^{\mathrm{CIS(D_\infty)}}(\omega))^\dagger + \mathcal{H}^{\mathrm{CIS(D_\infty)}}(\omega)) \tag{114}$$

2.C. Model System. The Hubbard model offers one of the simplest ways to get insight into how the interactions between electrons can give rise to insulating, doped, and conducting effects in a solid. In this work, we take a finite 1D Hubbard model (without periodic boundary conditions) as our testing system, which is described by the Hamiltonian

$$\mathcal{H} \equiv \tau \sum_{\langle\mu\nu\rangle} (a_\mu^\dagger a_\nu + \overline{a}_\mu^\dagger \overline{a}_\nu) + V_\mu \sum_\mu (a_\mu^\dagger a_\mu + \overline{a}_\mu^\dagger \overline{a}_\mu) + U \sum_\mu a_\mu^\dagger \overline{a}_\mu^\dagger a_\mu \overline{a}_\mu \tag{115}$$

where μ denotes the site of the system; τ is the hopping integral between neighboring sites, V_μ is the on-site energy (for site μ), and U is the repulsion energy between two electrons of opposite spin occupying the same site μ. (Here we keep the repulsion energy the same for all sites.) A bar indicates spin down. Note that for all of the calculations below, we calculate only the excitation energy of the first and second excited singlet states and we set $\eta = 0$ in eq 64. Note also that, for this model problem, $W^p(\mathbf{r}, \mathbf{r}')$ (eq 55) is replaced by $W^p_{\mu\mu\nu\nu}$ (eq 65).

3. RESULTS

We apply the theory above to an eight-site 1D Hubbard model, and we assume half-filling with eight electrons. The hopping integral between neighboring sites τ is set to be 1.0 for all systems, while the electron repulsion energy U is varied. All quantities will be calculated in au henceforward. The exact excitation energies are obtained by diagonalizing the Hamiltonian with direct diagonalization.

3.A. Metallic System. We first study metallic systems. In metallic systems, every site has the same on-site energy ($V_\mu = 0$ for all sites μ).[51] The electron repulsion energy U is varied from 0 to 0.7. Results are shown in Figure 3. One can see that for this system none of these approximated methods gives perfect results. For both excited states, all of the CI methods underestimate the energy, and TDHF gives the largest negative errors here. Note that CIS generates larger negative errors compared with correlated CI methods. We believe that this failure is really a failure of the HF calculation, which overestimates the ground-state energy: the difference between the exact ground-state energy and the answer given by HF is as large as 0.08. In general, CIS is known to overestimate the excitation energy.[47,52] Pertubatively including the double-excitations gives slightly better results but still with an error as large as −0.02. Although the BSE-TDA method generally overestimates the energy (except for $U = 0.7$), this method gives relatively smaller errors compared to CI methods. The BSE-RPA method generates the most accurate results for small U values but underestimates the energy when U gets larger (e.g., when $U = 0.6$ and 0.7 for S_1 and $U = 0.7$ for S_2).

3.B. Doped Impurity Systems. By lowering the energy of a single site in the metallic system, one can model an impurity. This dopes an otherwise metallic system[51] and can influence the overall photoactivitiy or electrical properties of the total system.

DOI: 10.1021/acs.jctc.7b00246
J. Chem. Theory Comput. XXXX, XXX, XXX−XXX

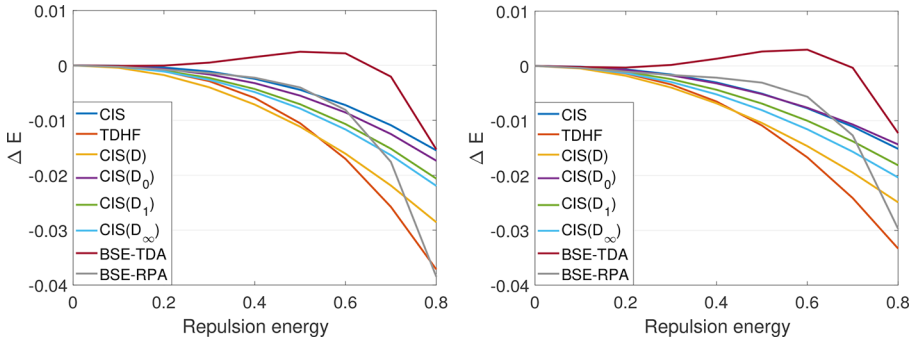

Figure 5. Errors for the excitation energy of the first (left, S_1) and second (right, S_2) excited singlet states for the "molecular" system ($V_{even} = -0.5$, $V_{odd} = 0$, $\tau = 1.0$). All errors are relative to the exact diagonalization. BSE-TDA maintains the same tendency and provides the smallest error when U reaches its maximum. BSE-RPA underestimates the energy too much for large U. Higher-level CI approaches give worse results compared to CIS.

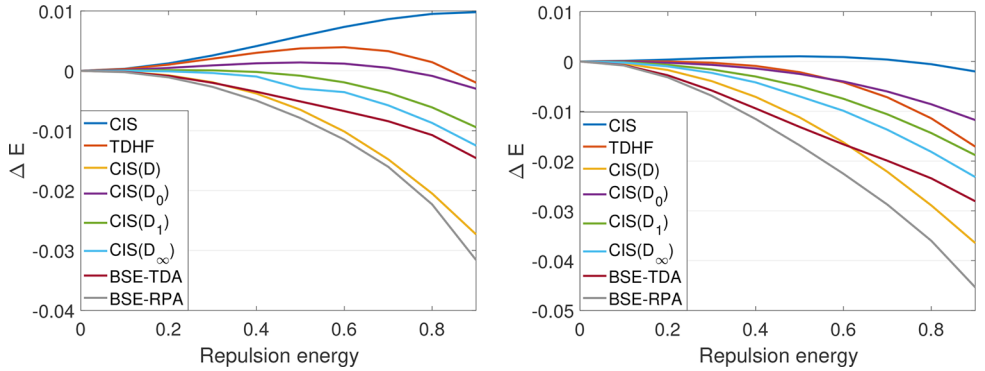

Figure 6. Errors for the excitation energy of the first (left, S_1) and second (right, S_2) excited singlet states for the "molecular" system ($V_{even} = -1.0$, $V_{odd} = 0$, $\tau = 1.0$). All errors are relative to the exact diagonalization. CIS overestimates the energy for S_1 but gives the most accurate results for S_2. BSE-TDA is only better than CIS(D) and BSE-RPA, which generates the largest error in this case.

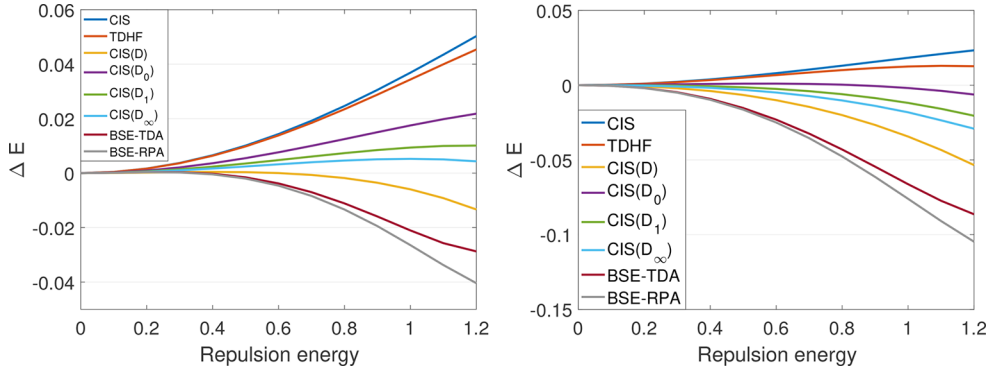

Figure 7. Errors for the excitation energy of the first (left, S_1) and second (right, S_2) excited singlet states for the "molecular" system ($V_{even} = -2.0$, $V_{odd} = 0$, $\tau = 1.0$). All errors are relative to the exact diagonalization. Both BSE methods underestimate the energy, while CIS and TDHF overestimate the energy. CIS(D_∞) gives the best results for S_1, and yet CIS(D_0) generates the best results for S_2.

In Figure 4, we calculate results for electron repulsion energies U between 0 and 0.7. Here the on-site energy V_μ is set to be −0.5. It can be seen in Figure 4 that the results are roughly identical to the metallic case: All of the CI methods underestimate the energy while BSE-TDA overestimates the energy (except for $U = 0.7$) for both excited states. The BSE-TDA method again yields a smaller error compared to CI approaches. BSE-RPA is accurate for small U values but gives large errors when U gets larger. The same conclusion holds for the case $V_\mu = -1.0$ (where the on-site energy is comparable with the hopping integral).

3.C. Molecular (Semiconducting/Insulating) Systems. To simulate a "molecular" Hubbard model, we construct an alternating Hamiltonian, whereby V_{even} is significantly lowered relative to $V_{odd} = 0$. In doing so, we expect that orbitals with lower energies will be doubly occupied and well separated from virtual orbitals. Thus, by creating an energy gap, we should be simulating closed-shell insulators and/or semiconductors (depending on the gap size).

For "molecular" systems with a small energy gap ($V_{even} = -0.5$), the electron repulsion energy U is varied from 0 to 0.8. As shown in Figure 5, the error given by the BSE-TDA method is further reduced, while the error of BSE-RPA increases. For the CI approaches, we find a very unusual result: the CIS energy outperforms the correlated methods. Clearly there is a nonintuitive cancellation of error in these calculations.

DOI: 10.1021/acs.jctc.7b00246
J. Chem. Theory Comput. XXXX, XXX, XXX−XXX

For "molecular" systems with an energy gap equal to the hopping integral ($V_{even} = -1.0$), Figure 6 demonstrates that our results are very different than all previous cases. Though CIS(D) still generates a large negative error, the CIS(D_n) approaches behave much better now. Interestingly, CIS(D_0) gives the best results in this case (and not CIS(D_∞)). The performance of the BSE-TDA method is no longer as good, though it is slightly better than CIS(D). The BSE-RPA is the worst and generates the largest error. Finally, CIS performs poorly for S_1 but quite well for S_2; again, there must be a nonintuitive cancellation of errors here.

Finally, we consider the final, extreme "molecular" case whereby the on-site energy difference is now twice as large as the hopping integral ($V_{even} = -2.0$). As Figure 7 shows, for S_1, CIS and TDHF generate quite large errors (as large as 0.05) as U increases from 0 to 1.2, overestimating the energy. CIS(D) and CIS(D_n) give smaller errors compared with the BSE methods as the latter underestimate the energy. CIS(D_∞) gives the most accurate results for S_1; however, surprisingly, CIS(D_0) provides the most accurate results for S_2. For S_2, CIS and TDHF also overestimate the energy, but the errors are smaller compared with S_1. BSE methods are not as reliable as CI methods in this case.

Overall, clearly BSE methods perform best for metallic and semiconducting systems, and CI methods perform best for insulating systems. That being said, though, there is no obvious pattern for identifying the exact performance of each specific algorithm.

4. DISCUSSION

The results above (in section 3) have compared CI methods versus BSE methods for calculating the excitation energy of the first and second excited singlet states. For all of the cases studied, we did not find a universally optimal approach that can generate relatively small errors for every system, though it is clear that the BSE-TDA method behaves better for metallic and semiconducting systems and gradually loses its advantage when the system becomes more "molecular". Here we analyze several aspects that affect the performance of BSE: (i) the reliability of the *GW* approximation, (ii) the influence of the screened correlation strength, and (iii) the effect of the non-self-consistent approximation (i.e., ignoring the frequency dependence of W^p) for BSE.

4.A. *GW* Approximation: Strengths and Weaknesses. In ref 40, we demonstrated that the *GW* method holds comparative advantages versus traditional quantum chemistry approaches for calculating the ionization potentials and electron affinities across a large range of Hubbard-like Hamiltonians. However, the same conclusion did not hold for all orbitals (unpublished); in fact, we found that *GW* can generate accurate orbital energies only for HOMO and LUMO for these model systems. To demonstrate this state of affairs, we consider the metallic system as an example and plot the *Z*-factor for the metallic system in Figure 8a. One can see in Figure 8a that only the HOMO and LUMO *Z*-factors are consistently very close to 1, indicating that the *GW* approximation works well for these two orbitals. For other orbitals, however, the *Z*-factor in some cases is much smaller than 1, which implies that a non-self-consistent G_0W_0 calculation cannot be reliable. To further demonstrate this, we plot the frequency dependence of the self-energy for HOMO and HOMO−3 at $U = 0.7$ in Figure 8b. According to ref 40, we express the dynamic part of the self-energy for HOMO and HOMO−3 as

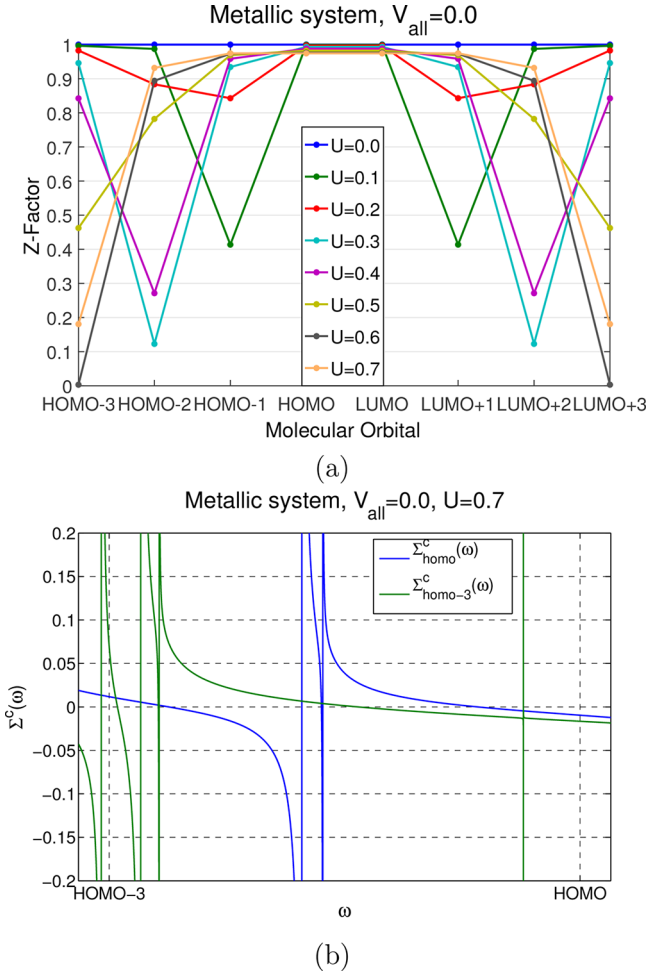

Figure 8. (a) *Z*-factors (eq 50) for the metallic systems and (b) the dynamic correlation part of the self-energy Σ^c (eq 116) as a function of ω for HOMO and HOMO−3 at $U = 0.7$. In (a), only the HOMO and LUMO *Z*-factors are consistently very close to 1 for any repulsion energy. In (b), $\Sigma^c_{homo}(\omega)$ is very flat and smooth at $\omega = \varepsilon_{homo}$, while $\Sigma^c_{homo-3}(\omega)$ is very sharp at $\omega = \varepsilon_{homo-3}$, indicating that *GW* (or, really, G_0W_0) will be meaningful for the HOMO but not for HOMO−3 when $U = 0.7$.

$$\Sigma^c_{pp}(\omega) = \sum_{jbkc}\sum_{I}\left(\sum_{i}\frac{(ip|jb)(ip|kc)}{\hbar\omega + \Omega_I^{TDH} - \varepsilon_i^H - i\eta} + \sum_{a}\frac{(ap|jb)(ap|kc)}{\hbar\omega - \Omega_I^{TDH} - \varepsilon_a^H + i\eta}\right)M^I_{jbkc} \quad (116)$$

where p = HOMO or HOMO−3. (Note that Ω_I^{TDH} in eq 116 corresponds to positive TDH eigenvalues.) It can been seen from Figure 8b that $\Sigma^c_{homo}(\omega)$ (blue line) is very flat and smooth at $\omega = \varepsilon_{homo}$, giving rise to a very small derivative $\frac{\partial\,\mathrm{Re}\,\Sigma^c(\varepsilon^H_{homo})}{\partial\omega}$. According to eq 50, the *Z*-factor for HOMO is therefore very close to 1. In contrast, $\Sigma^c_{homo-3}(\omega)$ is very sharp at $\omega = \varepsilon_{homo-3}$, leading to a very small *Z*-factor (~0.2 from Figure 8a), and indicating the failure of the *GW* approximation for HOMO−3 at $U = 0.7$. The same conclusion holds for doped and molecular systems.

In summary, the *GW* approximation works well when the quantities $-\Omega_I^{TDH} + \varepsilon_i^H$ and $\Omega_I^{TDH} + \varepsilon_a^H$ are far away from the Hartree orbital energies, which is true only for the HOMO and LUMO in our tested systems. (See eq 116.) Thus, as a

DOI: 10.1021/acs.jctc.7b00246
J. Chem. Theory Comput. XXXX, XXX, XXX−XXX

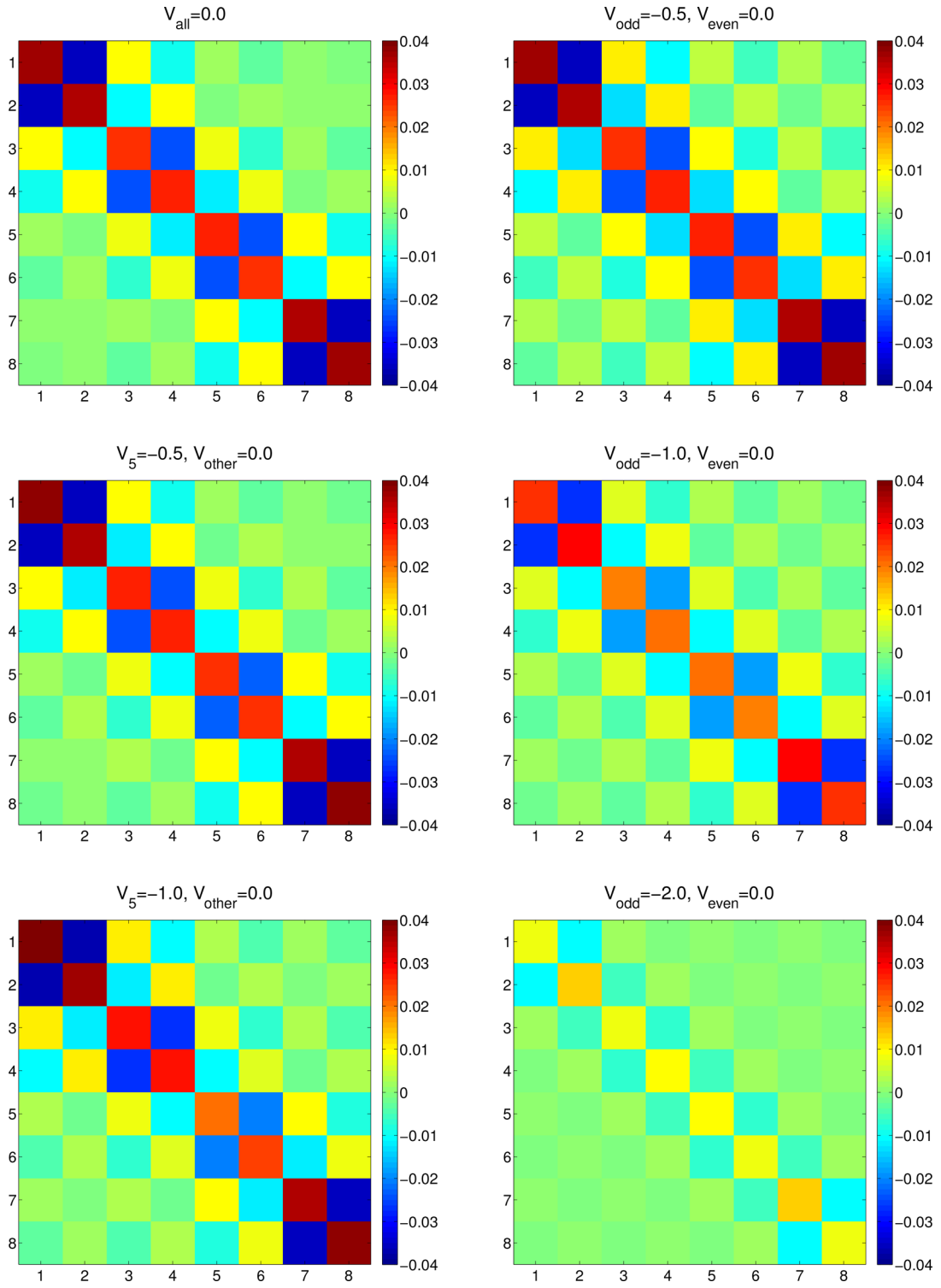

Figure 9. Dynamic screening effects for various 1D Hubbard chains. Here we plot $W^{p}_{\mu\mu\nu\nu}(\omega = 0)$ (eq 68). $U = 0.7$ for all systems. Note that the more insulating the system is, the less screening it shows. The screening of the extreme molecular system (bottom-right) is only one-third in strength compared to the metallic and doped systems.

compromise, we shifted the orbital energy by the same amount (eqs 51 and 52) when performing all BSE calculations. The BSE results might be improved in this paper if we can find more accurate quasiparticle energies.

4.B. Screened Correlation Effects. The strong performance of BSE-TDA for the metallic and the semiconducting systems in Figures 3−7 is consistent with the fact that BSE is popular in the solid-state community where screening is essential. To visualize screening, in Figure 9, we plot the dynamic screening interaction $W^{p}_{\mu\mu\nu\nu}$ for all systems, setting the repulsion energy to $U = 0.7$. As shown in Figure 9, the metallic system and doped systems (left panel) show more screening effects than the molecular systems (right panel), especially when the HOMO/LUMO gap is large. The effective screening for the extreme

DOI: 10.1021/acs.jctc.7b00246
J. Chem. Theory Comput. XXXX, XXX, XXX−XXX

molecular system (bottom-right) is only one-third in strength compared to that of the metallic and doped systems. This decrease in screening must degrade the performance of the BSE-TDA method. Future work must investigate whether this preliminary conclusions holds up for ab initio calculations or model problems with long-range Coulombic electron−electron repulsion energies (i.e., beyond the local interaction U of the Hubbard model).

4.C. Self-consistent and nonself-consistent BSE. Finally, a few words are in order about self-consistency. In this work, we have performed a non-self-consistent calculation for BSE by ignoring the frequency dependence of W^p, i.e., expressing K^d via eq 66. Alternatively, one can take the frequency dependence of W^p into account and apply the full expression of K^d (eq 47) to solve the BSE equation self-consistently. To compare the results, we have in fact performed several self-consistent calculations, and we find that for both TDA and RPA the self-consistent version and the non-self-consistent version of BSE generate almost exactly the same results. Thus, any BSE errors reported here are not from a lack of self-consistency.

5. CONCLUSIONS AND FUTURE DIRECTIONS

In this paper, we have reviewed BSE theory as well as a few widely used CI theories and we have systematically compared their performances for the calculation of the first two excitation energies for several finite 1D Hubbard chains. While BSE-RPA always underestimates the excitation energy for systems with large repulsion energy and behaves poorly compared with CI methods, BSE-TDA slightly outperforms the CI methods for metallic and semiconducting systems. For insulating molecular systems, BSE-TDA is not as accurate as CIS(D) and CIS(D_n). To explain these differences, the most obvious reason would be the choice of initial orbitals and orbital energies, Hartree or Hartree−Fock. Note that in this study our starting point is a direct Hartree calculation without any DFT functionals, and we have shown in ref 40 that these Hartree orbitals can be unreliable without any correction. Thus, there is always the question of whether BSE would be improved if more accurate quasiparticle energies can be obtained in some other fashion; recall that our GW calculations yield meaningful orbital corrections only for the HOMO and LUMO. We intend to address this question shortly.

In the future, several other questions must also be addressed. First, in order to make contact with the solid-state and materials literature, it will be essential to work with larger model systems. In such a case, in order to push finite Hubbard models beyond eight sites and recover exact excitation energies, one will need to implement a more sophisticated eigensolver, e.g., a density matrix renormalization solver.[53] Alternatively, it will also be crucial to implement periodic boundary conditions.

Second, as we have already demonstrated, the performance of BSE (relative to quantum chemistry CI methods) is inextricably tied to the strength of the screening tensor (i.e., how well one electron's charge is screened by the other electrons). For such a quantity, one may question whether the Hubbard model is the correct starting point for our analysis. How will our results change when we apply BSE and CI methods to truly ab initio calculations or model problems with long-range Coulombic forces, where the screening tensor may look very different from the present article?

Both of these outstanding questions will be addressed in a future publication.

APPENDIX A

Here we give a brief derivation of eq 4a starting from eq 3. To derive eqs 4a and 4b, we first apply an external time-local one-electron potential $\tilde{u}(\mathbf{x}_2, \mathbf{x}_2'; t)$. In the formulation of second quantization, assuming a Schrödinger representation, this potential takes the form

$$\hat{H}_S^{\text{ext}}(t_2) = \int d\mathbf{x}_2' \int d\mathbf{x}_2\, \hat{\Psi}^\dagger(\mathbf{x}_2)\tilde{u}(\mathbf{x}_2, \mathbf{x}_2'; t_2)\hat{\Psi}(\mathbf{x}_2') \tag{A1}$$

Vice versa, if we define a quantity $u(\mathbf{x}_2, t_2; \mathbf{x}_2', t_2') = \tilde{u}(\mathbf{x}_2, \mathbf{x}_2'; t_2)\delta(t_2 - t_2')$, we may write

$$\hat{H}_S^{\text{ext}}(t_2) = \int d\mathbf{x}_2' \int d\mathbf{x}_2 \int dt_2'\, \hat{\Psi}^\dagger(\mathbf{x}_2)u(\mathbf{x}_2, t_2; \mathbf{x}_2', t_2')\hat{\Psi}(\mathbf{x}_2') \tag{A2}$$

For shorthand, as usual, we will now denote $u(2, 2') \equiv u(\mathbf{x}_2, t_2; \mathbf{x}_2', t_2')$.

Now, the total Hamiltonian is $\hat{H}_{\text{total}} = \hat{H} + \hat{H}^{\text{ext}}$, where $\hat{H}$ is the standard time-independent electronic Hamiltonian that includes all Coulomb interactions. In the interaction picture, the external applied Hamiltonian becomes

$$\hat{H}_I^{\text{ext}}(t_2) = e^{i\hat{H}t_2}\hat{H}_S^{\text{ext}}e^{-i\hat{H}t_2} \tag{A3}$$

$$= \int d\mathbf{x}_2' \int d\mathbf{x}_2 \int dt_2'\, \hat{\Psi}^\dagger(\mathbf{x}_2, t_2)u(2, 2')\hat{\Psi}(\mathbf{x}_2', t_2') \tag{A4}$$

At this point, if we invoke the adiabatic Gell-Mann and Low theorem,[55] we find that the one- and two-particle Green's functions can be written as

$$G_1(1, 1') = -\frac{i}{\hbar}\frac{\langle N_0|T[\hat{S}\hat{\Psi}(1)\hat{\Psi}^\dagger(1')]|N_0\rangle}{\langle N_0|T[\hat{S}]|N_0\rangle} \tag{A5}$$

$$G_2(12; 1'2') = \left(-\frac{i}{\hbar}\right)^2\frac{\langle N_0|T[\hat{S}\hat{\Psi}(1)\hat{\Psi}(2)\hat{\Psi}^\dagger(2')\hat{\Psi}^\dagger(1')]|N_0\rangle}{\langle N_0|T[\hat{S}]|N_0\rangle} \tag{A6}$$

Here we have replaced $|N\rangle$ (the true many-body ground state) by $|N_0\rangle$ (the ground state without any applied perturbation). The function $\hat{S}$ is defined by

$$\hat{S} = \exp\left[-\frac{i}{\hbar}\int_{-\infty}^{\infty} dt_2\, \hat{H}_I^{\text{ext}}(t_2)\right] \tag{A7}$$

$$= \exp\left[-\frac{i}{\hbar}\int_{-\infty}^{\infty} d2\, \hat{\Psi}^\dagger(2)u(2, 2')\hat{\Psi}(2)\right] \tag{A8}$$

In all expressions above, $\hat{T}$ denotes time ordering.

Finally, it is straightforward to derive eq 4a in the paper. From eqs A5 and A6, it is clear that the functional differential of $G_1(1, 1')$ is

$$\delta G_1(1, 1') = -\frac{i}{\hbar}\frac{\langle N_0|T[\delta\hat{S}\hat{\Psi}(1)\hat{\Psi}^\dagger(1')]|N_0\rangle}{\langle N_0|T[\hat{S}]|N_0\rangle} - G_1(1, 1')\frac{\langle N_0|T[\delta\hat{S}]|N_0\rangle}{\langle N_0|T[\hat{S}]|N_0\rangle} \tag{A9}$$

Furthermore, to evaluate $\delta\hat{S}$, we differentiate eq A8 and find

$$\delta\hat{S} = -\frac{i}{\hbar}\hat{T}\int d2\, d2'\, \hat{\Psi}^\dagger(2)\delta u(2, 2')\delta(2, 2')\hat{\Psi}(2') \tag{A10}$$

DOI: 10.1021/acs.jctc.7b00246
J. Chem. Theory Comput. XXXX, XXX, XXX−XXX

and therefore

$$\delta G_1(1, 1') = \int \mathrm{d}2\, \mathrm{d}2'\, \delta u(2, 2')[-G_2(12; 1'2'^+) + G_1(1, 1')G_1(2, 2'^+)] \quad \text{(A11)}$$

Note that we have added a positive sign to the t_2' time index to ensure the correct ordering of field operators. The functional derivative of $G_1(1, 1')$ with respect to $u(2, 2')$ is thus

$$\frac{\delta G_1(1, 1')}{\delta u(2, 2')} = -G_2(12; 1'2'^+) + G_1(1, 1')G_1(2, 2'^+) \quad \text{(A12)}$$

which completes the derivation of eq 4b. Finally, to derive eq 4a, we simply insert the definition $u(2, 2') \equiv u(\mathbf{x}_2, t_2; \mathbf{x}_2', t_2') = \tilde{u}(\mathbf{x}_2, \mathbf{x}_2'; t_2)\delta(t_2 - t_2')$, integrate over t_2', and take the derivative

$$\frac{\delta G_1(1, 1')}{\delta \tilde{u}(\mathbf{x}_2, \mathbf{x}_2'; t_2)}.$$

AUTHOR INFORMATION

Corresponding Author

*E-mail: subotnik@sas.upenn.edu. Phone: (215)746-7078.

ORCID

Qi Ou: 0000-0002-6400-7522

Present Address

†Q.O.: Department of Mechanical and Aerospace Engineering, Princeton University, Princeton, NJ 08544-5263.

Funding

This work was supported by NSF CAREER Grant CHE-1150851. J.E.S. gratefully acknowledges support from the Stanford PULSE Institute and a John Simon Guggenheim Memorial fellowship.

Notes

The authors declare no competing financial interest.

ACKNOWLEDGMENTS

The authors thank Leeor Kronik for very useful conversations.

REFERENCES

(1) Foresman, J. B.; Head-Gordon, M.; Pople, J. A.; Frisch, M. J. Toward a Systematic Molecular Orbital Theory for Excited States. *J. Phys. Chem.* **1992**, *96*, 135−149.

(2) Stratmann, R. E.; Scuseria, G. E.; Frisch, M. J. An efficient implementation of time-dependent density-functional theory for the calculation of excitation energies of large molecules. *J. Chem. Phys.* **1998**, *109*, 8218−8224.

(3) Onida, G.; Reining, L.; Rubio, A. Electronic excitations: density-functional versus many-body Green's-function approaches. *Rev. Mod. Phys.* **2002**, *74*, 601−659.

(4) Adler, D.; Feinleib, J. Electrical and Optical Properties of Narrow-Band Materials. *Phys. Rev. B* **1970**, *2*, 3112−3134.

(5) Scholes, G. D. Long-Range Resonance Energy Transfer in Molecular Systems. *Annu. Rev. Phys. Chem.* **2003**, *54*, 57−87.

(6) Autschbach, J.; Ziegler, T.; van Gisbergen, S. J. A.; Baerends, E. J. Chiroptical properties from time-dependent density functional theory. I. Circular dichroism spectra of organic molecules. *J. Chem. Phys.* **2002**, *116*, 6930−6940.

(7) Chang, E.; Bussi, G.; Ruini, A.; Molinari, E. Excitons in Carbon Nanotubes: An *Ab Initio* Symmetry-Based Approach. *Phys. Rev. Lett.* **2004**, *92*, 196401.

(8) Spataru, C. D.; Ismail-Beigi, S.; Capaz, R. B.; Louie, S. G. Theory and *Ab Initio* Calculation of Radiative Lifetime of Excitons in Semiconducting Carbon Nanotubes. *Phys. Rev. Lett.* **2005**, *95*, 247402.

(9) Lopez-Acevedo, O.; Tsunoyama, H.; Tsukuda, T.; Häkkinen, H.; Aikens, C. M. Chirality and Electronic Structure of the Thiolate-Protected Au_{38} Nanocluster. *J. Am. Chem. Soc.* **2010**, *132*, 8210−8218.

(10) Gierschner, J.; Cornil, J.; Egelhaaf, H.-J. Optical Bandgaps of π-Conjugated Organic Materials at the Polymer Limit: Experiment and Theory. *Adv. Mater.* **2007**, *19*, 173−1912.

(11) Elward, J. M.; Irudayanathan, F. J.; Nangia, S.; Chakraborty, A. Optical Signature of Formation of Protein Corona in the Firefly Luciferase-CdSe Quantum Dot Complex. *J. Chem. Theory Comput.* **2014**, *10*, 5224−5228.

(12) Berkelbach, T. C.; Hybertsen, M. S.; Reichman, D. R. Bright and dark singlet excitons via linear and two-photon spectroscopy in monolayer transition-metal dichalcogenides. *Phys. Rev. B: Condens. Matter Mater. Phys.* **2015**, *92*, 085413.

(13) Kronik, L.; Neaton, J. B. Excited-State Properties of Molecular Solids from First Principles. *Annu. Rev. Phys. Chem.* **2016**, *67*, 587−616.

(14) Yarkony, D. R. Nonadiabatic effects in the vicinity of multiple surface crossings. Evaluation of derivative couplings with respect to rotational and internal degrees of freedom. Application to the charge transfer reaction H^++NO → H+NO^+. *J. Chem. Phys.* **1989**, *90*, 1657−1665.

(15) Yarkony, D. R. On the consequences of nonremovable derivative couplings 0.1. The geometric phase and quasidiabatic states: A numerical study. *J. Chem. Phys.* **1996**, *105*, 10456−10461.

(16) Matsika, S.; Yarkony, D. R. Spin-orbit coupling and conical intersections in molecules with an odd number of electrons. III. A perturbative determination of the electronic energies, derivative couplings and a rigorous diabatic representation near a conical intersection. *J. Chem. Phys.* **2002**, *116*, 2825−2835.

(17) Dallos, M.; Lischka, H.; Shepard, R.; Yarkony, D. R.; Szalay, P. G. Analytic evaluation of nonadiabatic coupling terms at the MR-CI level. II. Minima on the crossing seam: Formaldehyde and the photodimerization of ethylene. *J. Chem. Phys.* **2004**, *120*, 7330−7339.

(18) Marques, M. A.; Maitra, N. T.; Nogueira, F. M.; Gross, E.; Rubio, A. *Fundamentals of Time-Dependent Density Functional Theory*; Springer Science & Business Media: Berlin, Germany, 2012.

(19) Ullrich, C. A. *Time-Dependent Density-Functional Theory: Concepts and Applications*; Oxford University Press: New York, 2012.

(20) Bene, J. E. D.; Ditchfield, R.; Pople, J. A. Self-Consistent Molecular Orbital Methods. X. Molecular Orbital Studies of Excited States with Minimal and Extended Basis Sets. *J. Chem. Phys.* **1971**, *55*, 2236−2241.

(21) McLachlan, A. D.; Ball, M. A. Time-Dependent Hartree-Fock Theory for Molecules. *Rev. Mod. Phys.* **1964**, *36*, 844−855.

(22) Head-Gordon, M.; Rico, R. J.; Oumi, M.; Lee, T. J. A doubles correction to electronic excited states from configuration interaction in the space of single substitutions. *Chem. Phys. Lett.* **1994**, *219*, 21−29.

(23) Head-Gordon, M.; Grana, A. M.; Maurice, D.; White, C. A. Analysis of Electronic Transitions as the Difference of Electron Attachment and Detachment Densities. *J. Phys. Chem.* **1995**, *99*, 14261−14270.

(24) Christiansen, O.; Koch, H.; Jørgensen, P. The second-order approximate coupled cluster singles and doubles model CC2. *Chem. Phys. Lett.* **1995**, *243*, 409−418.

(25) Christiansen, O.; Koch, H.; Jørgensen, P.; Helgaker, T. Integral direct calculation of CC2 excitation energies: singlet excited states of benzene. *Chem. Phys. Lett.* **1996**, *263*, 530−539.

(26) Schirmer, J. Beyond the random-phase approximation: A new approximation scheme for the polarization propagator. *Phys. Rev. A: At., Mol., Opt. Phys.* **1982**, *26*, 2395−2416.

(27) Trofimov, A. B.; Schirmer, J. An efficient polarization propagator approach to valence electron excitation spectra. *J. Phys. B: At., Mol. Opt. Phys.* **1995**, *28*, 2299−2324.

(28) Head-Gordon, M.; Oumi, M.; Maurice, D. Quasidegenerate second-order perturbation corrections to single excitation configuration inter action. *Mol. Phys.* **1999**, *96*, 593−602.

(29) Heyd, J.; Scuseria, G. E. Efficient hybrid density functional calculations in solids: Assessment of the HeydScuseriaErnzerhof

DOI: 10.1021/acs.jctc.7b00246
J. Chem. Theory Comput. XXXX, XXX, XXX−XXX

screened Coulomb hybrid functional. *J. Chem. Phys.* **2004**, *121*, 1187−1192.
(30) Aufray, B.; Kara, A.; Vizzini, S.; Oughaddou, H.; Léandri, C.; Ealet, B.; Le Lay, G. Graphene-like silicon nanoribbons on Ag(110): A possible formation of silicene. *Appl. Phys. Lett.* **2010**, *96*, 183102.
(31) Mosconi, E.; Amat, A.; Nazeeruddin, M. K.; Grätzel, M.; De Angelis, F. First-Principles Modeling of Mixed Halide Organometal Perovskites for Photovoltaic Applications. *J. Phys. Chem. C* **2013**, *117*, 13902−13913.
(32) Fuchs, F.; Bechstedt, F. Indium-oxide polymorphs from first principles: Quasiparticle electronic states. *Phys. Rev. B: Condens. Matter Mater. Phys.* **2008**, *77*, 155107.
(33) Aryasetiawan, F.; Gunnarsson, O. The GW method. *Rep. Prog. Phys.* **1998**, *61*, 237.
(34) Hedin, L. On Correlation Effects in Electron Spectroscopies and the GW Approximation. *J. Phys.: Condens. Matter* **1999**, *11*, R489.
(35) Rohlfing, M.; Louie, S. G. Electron-hole excitations and optical spectra from first principles. *Phys. Rev. B: Condens. Matter Mater. Phys.* **2000**, *62*, 4927−4943.
(36) Rabani, E.; Baer, R.; Neuhauser, D. Time-dependent stochastic Bethe-Salpeter approach. *Phys. Rev. B: Condens. Matter Mater. Phys.* **2015**, *91*, 235302.
(37) Neuhauser, D.; Gao, Y.; Arntsen, C.; Karshenas, C.; Rabani, E.; Baer, R. Breaking the Theoretical Scaling Limit for Predicting Quasiparticle Energies: The Stochastic *GW* Approach. *Phys. Rev. Lett.* **2014**, *113*, 076402.
(38) Hedin, L. New Method for Calculating the One-Particle Green's Function with Application to the Electron-Gas Problem. *Phys. Rev.* **1965**, *139*, A796−A823.
(39) Salpeter, E. E.; Bethe, H. A. A Relativistic Equation for Bound-State Problems. *Phys. Rev.* **1951**, *84*, 1232−1242.
(40) Ou, Q.; Subotnik, J. E. Comparison between GW and Wave-Function-Based Approaches: Calculating the Ionization Potential and Electron Affinity for 1D Hubbard Chains. *J. Phys. Chem. A* **2016**, *120*, 4514−4525.
(41) Strinati, G. Application of the Green's Function Method to the Study of the Optical Properties of Semiconductors. *Riv. Nuovo Cim.* **1988**, *11*, 1.
(42) Note that if we express the time-dependent creation and annihilation operator as $\hat{\psi}(\mathbf{x}, t) = e^{iHt}\hat{\psi}(\mathbf{x})e^{-iHt}$ and $\hat{\psi}^{\dagger}(\mathbf{x}, t) = e^{iHt/\hbar}\hat{\psi}^{\dagger}(\mathbf{x})e^{-iHt/\hbar}$, we can rewrite χ_S^{eh} and $\tilde{\chi}_S^{eh}$ as

$$\chi_S^{eh}(\mathbf{x}_1, \mathbf{x}_2; t_1 - t_2) = \langle N|\hat{\psi}(\mathbf{x}_1)e^{-iH(t_1-t_2)/\hbar}\hat{\psi}^{\dagger}(\mathbf{x}_2)|N_S\rangle \exp[i(E_S + E_0)(t_1 - t_2)/2\hbar]$$

$$\tilde{\chi}_S^{eh}(\mathbf{x}_1, \mathbf{x}_2; t_1 - t_2) = \langle N_S|\hat{\psi}(\mathbf{x}_1)e^{-iH(t_1-t_2)/\hbar}\hat{\psi}^{\dagger}(\mathbf{x}_2)|N\rangle \exp[-i(E_S + E_0)(t_1 - t_2)/2\hbar]$$

for $t_1 > t_2$ and

$$\chi_S^{eh}(\mathbf{x}_1, \mathbf{x}_2; t_1 - t_2) = -\langle N|\hat{\psi}^{\dagger}(\mathbf{x}_2)e^{-iH(t_2-t_1)/\hbar}\hat{\psi}(\mathbf{x}_1)|N_S\rangle \exp[i(E_S + E_0)(t_2 - t_1)/2\hbar]$$

$$\tilde{\chi}_S^{eh}(\mathbf{x}_1, \mathbf{x}_2; t_1 - t_2) = -\langle N_S|\hat{\psi}^{\dagger}(\mathbf{x}_2)e^{-iH(t_2-t_1)/\hbar}\hat{\psi}(\mathbf{x}_1)|N\rangle \exp[-i(E_S + E_0)(t_2 - t_1)/2\hbar]$$

for $t_1 < t_2$. This representation proves that χ_S^{eh} and $\tilde{\chi}_S^{eh}$ are functions of only $t_1 - t_2$.
(43) For G^{III} and G^{IV}, we must have $t_2 > t_2'$ or $t_2 < t_2'$, and therefore, the limit of $t_2' = t_2 + \delta$ is not meaningful.
(44) Inkson, J. C. *Many-Body Theory of Solids: An Introduction*; Plenum Press: New York, 1984.
(45) Bruneval, F.; Gonze, X. Accurate *GW* self-energies in a plane-wave basis using only a few empty states: Towards large systems. *Phys. Rev. B: Condens. Matter Mater. Phys.* **2008**, *78*, 085125.
(46) Furche, F. On the density matrix based approach to time-dependent density functional response theory. *J. Chem. Phys.* **2001**, *114*, 5982−5992.
(47) Dreuw, A.; Head-Gordon, M. Single reference ab initio methods for the calculation of excited states of large molecules. *Chem. Rev.* **2005**, *105*, 4009.
(48) Hättig, C. Structure Optimizations for Excited States with Correlated Second-Order Methods: CC2 and ADC(2). *Adv. Quantum Chem.* **2005**, *50*, 37−60.
(49) Purvis, G. D., III; Bartlett, R. J. A full coupled-cluster singles and doubles model: The inclusion of disconnected triples. *J. Chem. Phys.* **1982**, *76*, 1910−1918.
(50) One should note that the terms introduced via the transformation on $\hat{H}_0$ in CC2 contribute to only the third and higher orders to the excitation energies of single-excitation dominated transitions. To obtain the excitation energies correct through the second order, this transformation can safely be discarded.
(51) In truth, it can be shown that an infinite half-filled Hubbard chain is always insulating.[54] Thus, formally, any "metallic" features of this Hubbard chain exist only because of the chain's finite size. That being said, the main conclusions presented here continue to hold if we consider a chain with less than half filling.
(52) Subotnik, J. E. Communication: Configuration interaction singles has a large systematic bias against charge-transfer states. *J. Chem. Phys.* **2011**, *135*, 071104.
(53) Chan, G. K.-L.; Sharma, S. The Density Matrix Renormalization Group in Quantum Chemistry. *Annu. Rev. Phys. Chem.* **2011**, *62*, 465−481.
(54) Lieb, E. H.; Wu, F. Y. Absence of Mott Transition in an Exact Solution of the Short-Range, One-Band Model in One Dimension. *Phys. Rev. Lett.* **1968**, *20*, 1445−1448.
(55) Fetter, A. L.; Walecka, J. D. *Quantum Theory of Many-article Systems*; Dover Publications, Inc.: New York, 2003.
(56) Note that we are not including here the Fourier transform of the first term on the right-hand side of eq 14. This term has been omitted because there is no residue at $\hbar\omega = E_s - E_0$.

DOI: 10.1021/acs.jctc.7b00246
J. Chem. Theory Comput. XXXX, XXX, XXX−XXX